# Regions for Asymptotic Expansions of Amplitudes

*Yao Ma*
*Institute for Theoretical Physics, ETH Zurich*

---

*DESY Theory Seminar*

*November 11th, 2024*

# *Asymptotic expansion of Feynman integrals*

- Evaluating multi-loop Feynman integrals poses significant challenges.

- For Feynman integrals with multiple scales in the external kinematics, a natural idea is to consider the asymptotic expansion.

$$\mathcal{A} \sim \mathcal{A}_0 + \left(\frac{\Lambda_{\text{small}}}{\Lambda_{\text{large}}}\right) \mathcal{A}_1 + \left(\frac{\Lambda_{\text{small}}}{\Lambda_{\text{large}}}\right)^2 \mathcal{A}_2 + \dots$$

- Moreover, asymptotic expansion offers insights into the intricate infrared structure of gauge theory.

- There are various techniques of doing asymptotic expansions.

# *Asymptotic expansion of Feynman integrals*

- Evaluating multi-loop Feynman integrals poses significant challenges.

- For Feynman integrals with multiple scales in the external kinematics, a natural idea is to consider the asymptotic expansion.

$$\mathcal{A} \sim \mathcal{A}_0 + \left(\frac{\Lambda_{\text{small}}}{\Lambda_{\text{large}}}\right) \mathcal{A}_1 + \left(\frac{\Lambda_{\text{small}}}{\Lambda_{\text{large}}}\right)^2 \mathcal{A}_2 + \dots$$

- Moreover, asymptotic expansion offers insights into the intricate infrared structure of gauge theory.

- There are various techniques of doing asymptotic expansions.

***This talk: "the method of regions"***

# *The method of regions (MoR)*

- ***Statement:*** $\text{entire space} = R_1 \cup R_2 \cup \cdots \cup R_n$

$$\mathcal{I} = \mathcal{I}^{(R_1)} + \mathcal{I}^{(R_2)} + \cdots + \mathcal{I}^{(R_n)}.$$

***The original integral, $\mathcal{I}$ , can be restored by summing over contributions from the regions.***

# *The method of regions (MoR)*

- ***Statement:*** entire space $= R_1 \cup R_2 \cup \cdots \cup R_n$

$$\mathcal{I} = \mathcal{I}^{(R_1)} + \mathcal{I}^{(R_2)} + \cdots + \mathcal{I}^{(R_n)}.$$

***The original integral, $\mathcal{I}$, can be restored by summing over contributions from the regions.***

The MoR works for all known examples so far. However,

- There are no rigorous proofs yet.
- It is tricky to identify the regions: usually people use heuristic methods based on examples and experience.

# *The method of regions (MoR)*

Example: one-loop Sudakov form factor

(Becher, Broggio, Ferroglia 2014)

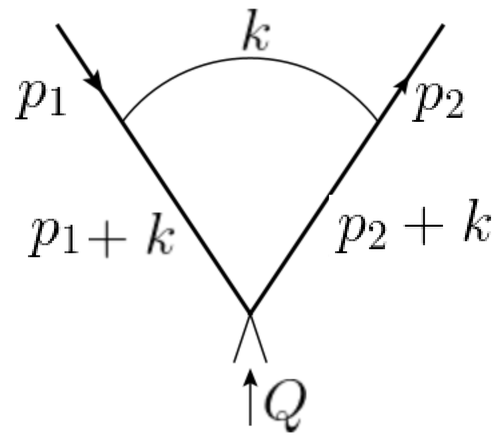


The on-shell limit kinematics

$$p_1^\mu \sim Q\ (\underset{+}{1},\ \underset{-}{\lambda},\ \underset{\perp}{\lambda^{1/2}}), \qquad p_2^\mu \sim Q\ (\underset{+}{\lambda},\ \underset{-}{1},\ \underset{\perp}{\lambda^{1/2}})$$

$$p_1^2/Q^2 \sim p_2^2/Q^2 \sim \lambda \to 0$$

# *The method of regions (MoR)*

Example: one-loop Sudakov form factor

(Becher, Broggio, Ferroglia 2014)

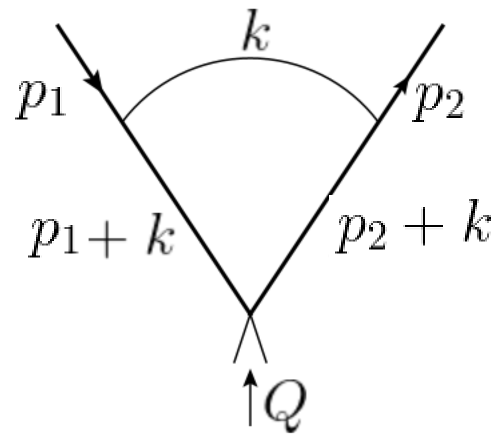


The on-shell limit kinematics

$$p_1^\mu \sim Q\;(\underset{+}{1},\ \underset{-}{\lambda},\ \underset{\perp}{\lambda^{1/2}}),\qquad p_2^\mu \sim Q\;(\underset{+}{\lambda},\ \underset{-}{1},\ \underset{\perp}{\lambda^{1/2}})$$

$$p_1^2/Q^2 \sim p_2^2/Q^2 \sim \lambda \to 0$$

The Feynman integral

$$\mathcal{I} = \mathcal{C} \cdot \int d^D k \frac{1}{(k^2 + i0)\,((p_1 + k)^2 + i0)\,((p_2 + k)^2 + i0)}$$

can be evaluated directly, or, we can apply the method of regions.

# The method of regions (MoR)

Step 1: identify **4** regions in total:

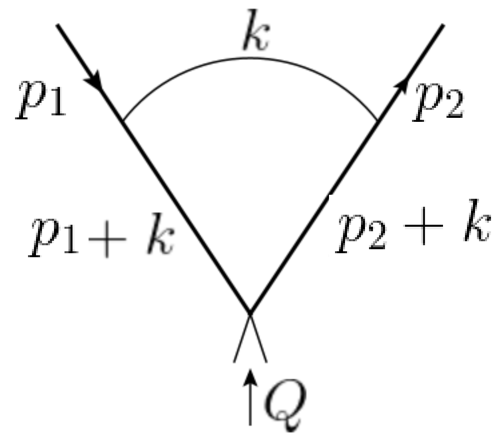


**Hard region:** $k^\mu \sim Q(1, 1, 1)$

**Collinear-1 region:** $k^\mu \sim Q(1, \lambda, \lambda^{1/2})$

**Collinear-2 region:** $k^\mu \sim Q(\lambda, 1, \lambda^{1/2})$

**Soft region:** $k^\mu \sim Q(\lambda, \lambda, \lambda)$

# The method of regions (MoR)

Step 1: identify **4** regions in total:

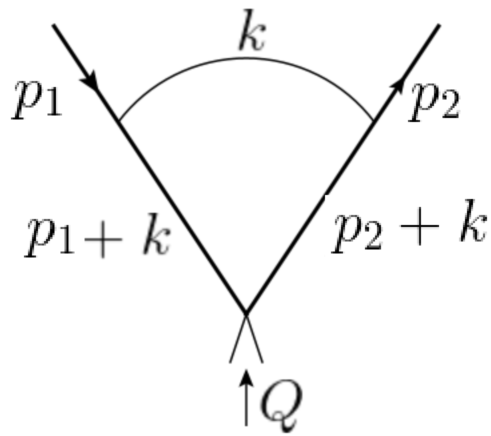


Hard region: $k^\mu \sim Q(1,1,1)$

Collinear-1 region: $k^\mu \sim Q(1,\lambda,\lambda^{1/2})$

Collinear-2 region: $k^\mu \sim Q(\lambda,1,\lambda^{1/2})$

Soft region: $k^\mu \sim Q(\lambda,\lambda,\lambda)$

Step 2: perform expansion around each region:

$$\mathcal{I}_H = \mathcal{C}\cdot\int d^Dk \frac{1}{(k^2+i0)\,(k^2+2p_1\cdot k+i0)\,(k^2+2p_2\cdot k+i0)}+\dots$$

$$\mathcal{I}_{C_1} = \mathcal{C}\cdot\int d^Dk \frac{1}{(k^2+i0)\,((p_1+k)^2+i0)\,(2p_2\cdot k+i0)}+\dots$$

$$\mathcal{I}_{C_2} = \mathcal{C}\cdot\int d^Dk \frac{1}{(k^2+i0)\,(2p_1\cdot k+i0)\,((p_2+k)^2+i0)}+\dots$$

$$\mathcal{I}_S = \mathcal{C}\cdot\int d^Dk \frac{1}{(k^2+i0)\,(2p_1\cdot k+p_1^2+i0)\,(2p_2\cdot k+p_2^2+i0)}+\dots$$

# *The method of regions (MoR)*

Step 1: ….

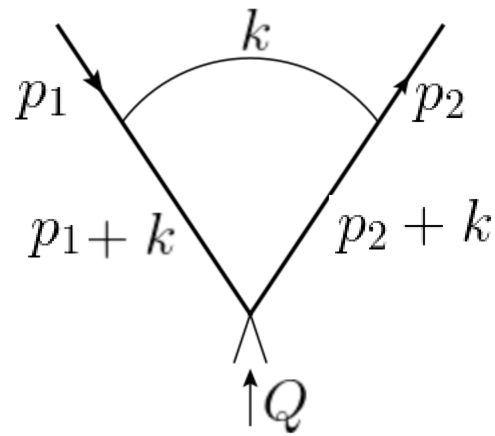


Step 2: ….

Step 3: sum over their contributions, and the original integral is reproduced:

$$\mathcal{I} = \mathcal{I}_H + \mathcal{I}_{C_1} + \mathcal{I}_{C_2} + \mathcal{I}_S = \frac{1}{Q^2}\left(\ln\frac{Q^2}{(-p_1^2)}\ln\frac{Q^2}{(-p_2^2)} + \frac{\pi^2}{3} + \ldots\right)$$

This equality holds to **all** orders of λ!

More examples are presented in Smirnov's book "*Applied Asymptotic Expansions in Momenta and Masses*".

# Parametric representation

The Lee-Pomeransky representation (Lee & Pomeransky 2013)

$$\mathcal{I}(G) = \frac{\Gamma(D/2)}{\Gamma((L+1)D/2-\nu)\prod_{e\in G}\Gamma(\nu_e)}\int_0^\infty \left(\prod_{e\in G} dx_e x_e^{\nu_e-1}\right)\left(\mathcal{P}\left(\boldsymbol{x},\boldsymbol{s}\right)\right)^{-D/2},$$

$$\mathcal{P}(\boldsymbol{x},\boldsymbol{s}) \equiv \mathcal{U}(\boldsymbol{x}) + \mathcal{F}(\boldsymbol{x},\boldsymbol{s}),$$

$$\mathcal{U}(\boldsymbol{x}) = \sum_{T^1}\prod_{e\notin T^1} x_e, \qquad \mathcal{F}(\boldsymbol{x},\boldsymbol{s}) = -\sum_{T^2} s_{T^2}\prod_{e\notin T^2} x_e + \mathcal{U}(\boldsymbol{x})\sum_e m_e^2 x_e\ .$$

**spanning trees** **spanning 2-trees**

# *Parametric representation*

The Lee-Pomeransky representation (Lee & Pomeransky 2013)

$$\mathcal{I}(G) = \frac{\Gamma(D/2)}{\Gamma((L+1)D/2-\nu)\prod_{e\in G}\Gamma(\nu_e)} \int_0^\infty \left(\prod_{e\in G} dx_e x_e^{\nu_e-1}\right) \left(\mathcal{P}\left(\boldsymbol{x},\boldsymbol{s}\right)\right)^{-D/2},$$

$$\mathcal{P}(\boldsymbol{x},\boldsymbol{s}) \equiv \mathcal{U}(\boldsymbol{x}) + \mathcal{F}(\boldsymbol{x},\boldsymbol{s}),$$

$$\mathcal{U}(\boldsymbol{x}) = \sum_{T^1}\prod_{e\notin T^1} x_e, \qquad \mathcal{F}(\boldsymbol{x},\boldsymbol{s}) = -\sum_{T^2} s_{T^2}\prod_{e\notin T^2} x_e + \mathcal{U}(\boldsymbol{x})\sum_e m_e^2 x_e \ .$$

**spanning trees** **spanning 2-trees**

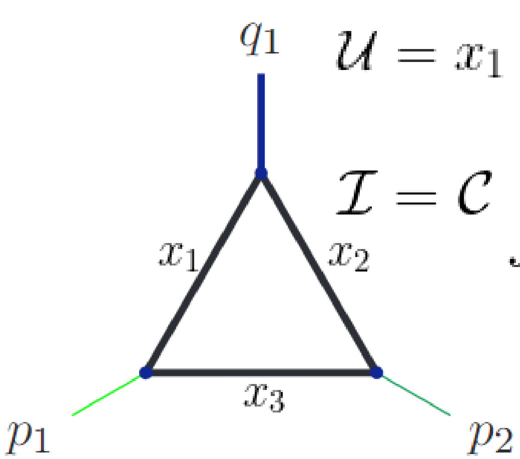


$$\mathcal{U} = x_1 + x_2 + x_3, \quad \mathcal{F} = (-p_1^2)x_1x_3 + (-p_2^2)x_2x_3 + (-q_1^2)x_1x_2$$

$$\mathcal{I} = \mathcal{C}\int_0^\infty dx_1dx_2dx_3 x_1^{\nu_1-1}x_2^{\nu_2-1}x_3^{\nu_3-1}$$

$$\cdot\left(x_1+x_2+x_3-p_1^2x_1x_3-p_2^2x_2x_3-q_1^2x_1x_2\right)^{-D/2}$$

# *Parametric representation*

The Lee-Pomeransky representation (Lee & Pomeransky 2013)

$$\mathcal{I}(G) = \frac{\Gamma(D/2)}{\Gamma((L+1)D/2-\nu)\prod_{e\in G}\Gamma(\nu_e)} \int_0^\infty \left(\prod_{e\in G} dx_e x_e^{\nu_e-1}\right) \left(\mathcal{P}\left(\boldsymbol{x},\boldsymbol{s}\right)\right)^{-D/2},$$

$$\mathcal{P}(\boldsymbol{x},\boldsymbol{s}) \equiv \mathcal{U}(\boldsymbol{x}) + \mathcal{F}(\boldsymbol{x},\boldsymbol{s}),$$

$$\mathcal{U}(\boldsymbol{x}) = \sum_{T^1} \prod_{e\notin T^1} x_e, \qquad \mathcal{F}(\boldsymbol{x},\boldsymbol{s}) = -\sum_{T^2} s_{T^2} \prod_{e\notin T^2} x_e + \mathcal{U}(\boldsymbol{x}) \sum_e m_e^2 x_e \ .$$

**spanning trees** **spanning 2-trees**

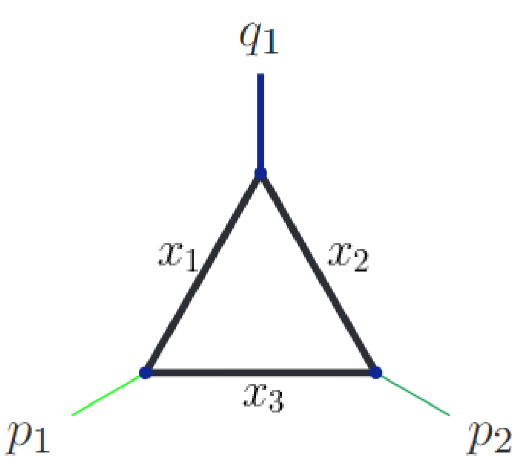


Each region → a certain scaling of the $\boldsymbol{x}$

$$\text{Hard region}: \ \boldsymbol{x_1, x_2, x_3 \sim \lambda^0}$$
$$\text{Collinear region to } p_1: \boldsymbol{x_1, x_3 \sim \lambda^{-1},\ x_2 \sim \lambda^0}$$
$$\text{Collinear region to } p_2: \boldsymbol{x_1 \sim \lambda^0, x_2, x_3 \sim \lambda^{-1}}$$
$$\text{Soft region}: \boldsymbol{x_1, x_2 \sim \lambda^{-1},\ x_3 \sim \lambda^{-2}}$$

# *Regions in different representations*

- Momentum space:

$$\text{Hard region: } k^\mu \sim Q(1,1,1)$$
$$\text{Collinear-1 region: } k^\mu \sim Q(1,\lambda,\lambda^{1/2})$$
$$\text{Collinear-2 region: } k^\mu \sim Q(\lambda,1,\lambda^{1/2})$$
$$\text{Soft region: } k^\mu \sim Q(\lambda,\lambda,\lambda)$$

- Parameter space:

$$\text{Hard region}: \; x_1, x_2, x_3 \sim \lambda^0$$
$$\text{Collinear region to } p_1: x_1, x_3 \sim \lambda^{-1}, \; x_2 \sim \lambda^0$$
$$\text{Collinear region to } p_2: x_1 \sim \lambda^0, x_2, x_3 \sim \lambda^{-1}$$
$$\text{Soft region}: x_1, x_2 \sim \lambda^{-1}, \; x_3 \sim \lambda^{-2}$$

- Relation between the scalings:

$$x_e \sim (D_e)^{-1}$$

# *Parametric representation*

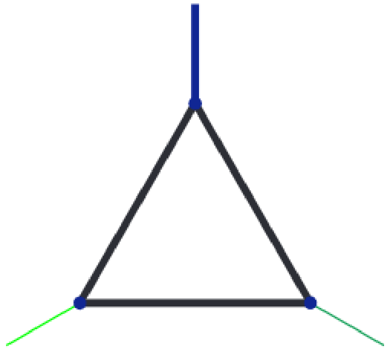


$$\text{Hard region}: \; x_1, x_2, x_3 \sim \lambda^0$$
$$\text{Collinear region to } p_1: x_1, x_3 \sim \lambda^{-1}, \; x_2 \sim \lambda^0$$
$$\text{Collinear region to } p_2: x_1 \sim \lambda^0, x_2, x_3 \sim \lambda^{-1}$$
$$\text{Soft region}: x_1, x_2 \sim \lambda^{-1}, \; x_3 \sim \lambda^{-2}$$

***Advantage of parametric representation: it provides a systematic way of identifying the regions using Newton polytope geometries.***

(Pak & Smirnov 2010; Jantzen, Smirnov, Smirnov, 2012.)

# *Identifying regions from Newton polytopes*

- Given the Lee-Pomeransky polynomial,

$$\mathcal{P}(\boldsymbol{x};\boldsymbol{s}) = \mathcal{U}(\boldsymbol{x}) + \mathcal{F}(\boldsymbol{x};\boldsymbol{s}),$$

  take the **exponents** of each term:

$$s x_1^{v_1} x_2^{v_2} \cdots x_n^{v_n} \to (v_1, v_2, \ldots, v_n; a) \quad \text{if} \quad s \sim \lambda^a Q^2$$

# *Identifying regions from Newton polytopes*

- Given the Lee-Pomeransky polynomial,

$$\mathcal{P}(\boldsymbol{x};\boldsymbol{s}) = \mathcal{U}(\boldsymbol{x}) + \mathcal{F}(\boldsymbol{x};\boldsymbol{s}),$$

take the **exponents** of each term:

$$s x_1^{v_1} x_2^{v_2} \cdots x_n^{v_n} \to (v_1, v_2, \ldots, v_n; a) \quad \text{if} \quad s \sim \lambda^a Q^2$$

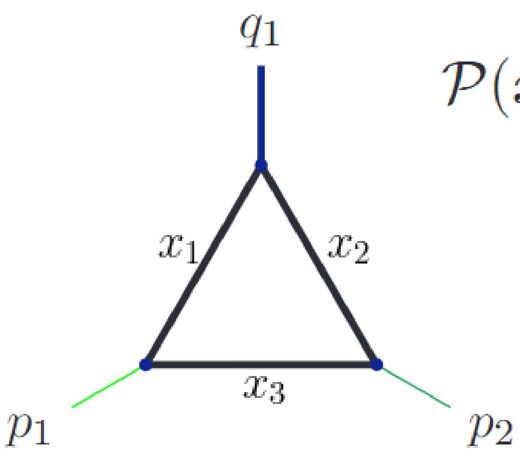


$$\mathcal{P}(\boldsymbol{x},\boldsymbol{s}) = x_1 + x_2 + x_3 - p_1^2 x_1 x_3 - p_2^2 x_2 x_3 - q_1^2 x_1 x_2$$

**(1,0,0;0)** **(0,1,0;0)** **(0,0,1;0)** **(1,0,1;1)** **(0,1,1;1)** **(1,1,0;0)**

Construct a Newton polytope, defined as the convex hull of the points.

**Regions <-> the lower facets of this Newton polytope.**

(Entries of the vector normal to a lower facet are precisely the scalings of $\boldsymbol{x_1}$, $\boldsymbol{x_2}$, ....)

# *Identifying regions from Newton polytopes*

**Regions <-> the lower facets of this Newton polytope**

Given a graph with $N$ propagators, the Newton polytope $\triangle$ is $N+1$ dimensional.

- **Facets:** the $N$-dimensional boundaries of $\triangle$.
- **Lower facets:** those facets whose inward-pointing normal vectors $\boldsymbol{v}$ satisfy $\boldsymbol{v}_{N+1}>0$.

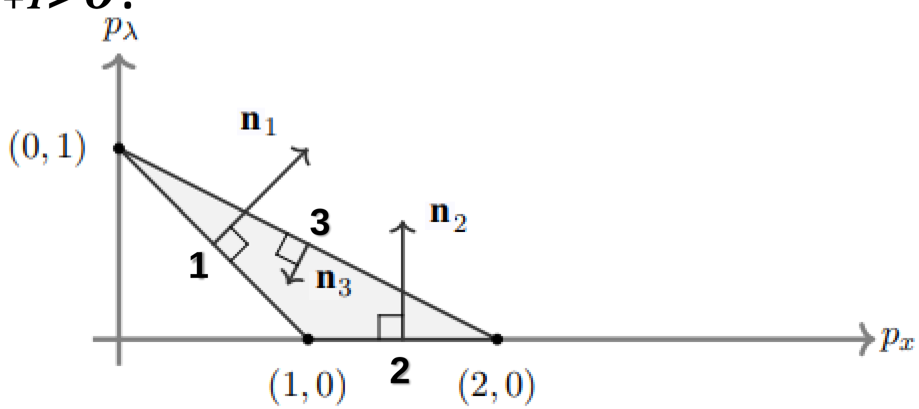


$1,2 \in F^+$

$3 \notin F^+$

- The vector $\boldsymbol{v}$ is usually referred to as the **region vector**, and its entries show the scaling of $\boldsymbol{x}$.

# *Identifying regions from Newton polytopes*

- There have been computer codes based on this approach:

  Asy2, ASPIRE, pySecDec, …

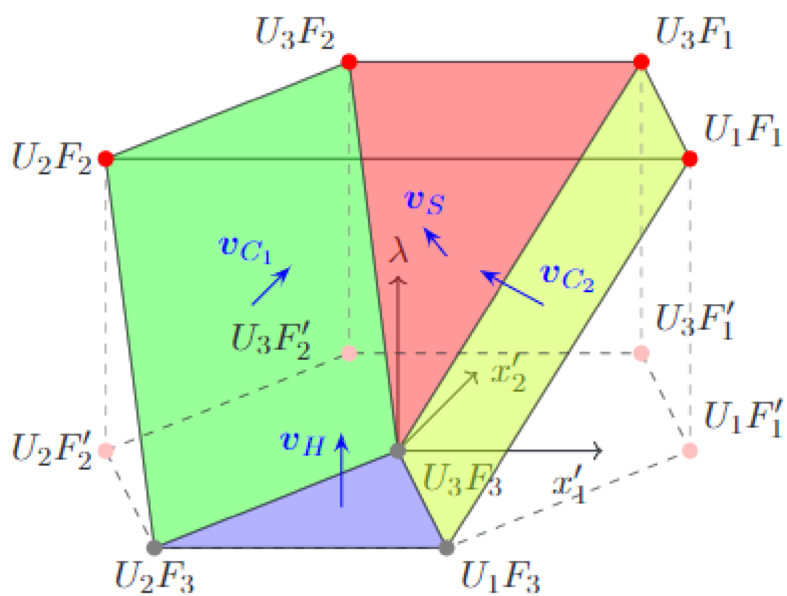


- Timely results may not be available if the graph is not too simple.

  Note that dim(polytope) = #(propagators)+1.

- Also, are there regions “hidden” inside the polytope?
- How should we interpret the output in momentum space?

# *Identifying regions from Newton polytopes*

- There have been computer codes based on this approach:

  Asy2, ASPIRE, pySecDec, …

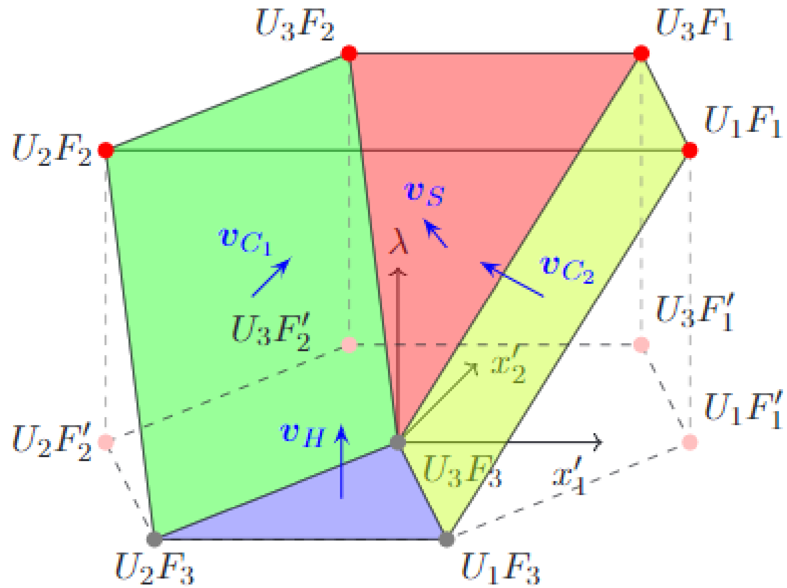


- ***Question: For any expansion of interest, can we establish a general rule, which governs all the regions and specifies all the relevant modes?***

# *Classification of the regions*

- **Actually, the Newton polytope approach may miss some regions.**
- **Two types of regions: "facet regions" and "hidden regions".**

√ ?

- **Most regions are facet regions.**
  - They correspond to lower facets of the Newton polytope.
  - They arise from singularities **at the endpoints** in parametric space.

- **Additionally, there may be hidden regions.**
  - They locate inside the Newton polytope.
  - They arise from singularities **away from endpoints** in parametric space.

# *Classification of the regions*

- **Actually, the Newton polytope approach may miss some regions.**
- **Two types of regions: "facet regions" and "hidden regions".**

√ ?

- **Most regions are facet regions.**
  - They correspond to lower facets of the Newton polytope.
  - They arise from singularities **at the endpoints** in parametric space.

→ **E.Gardi, F.Herzog, S.Jones, YM, J.Schlenk, JHEP07(2023)197.**

→ **YM, JHEP09(2024)197.**

→ **E.Gardi, F.Herzog, S.Jones, YM, in preparation.**

- **Additionally, there may be hidden regions.**
  - They locate inside the Newton polytope.
  - They arise from singularities **away from endpoints** in parametric space.

→ **E.Gardi, F.Herzog, S.Jones, YM, JHEP08(2024)127.**

# *The "on–shell expansion"*

- We start with the following asymptotic expansion:

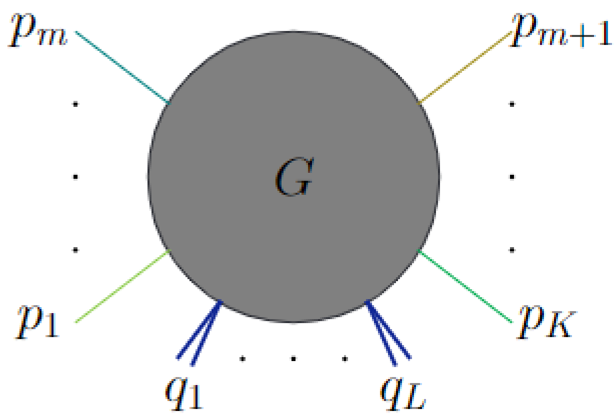


massless

$$p_i^2 \sim \lambda Q^2 \quad (i = 1, \ldots, K), \quad q_j^2 \sim Q^2 \quad (j = 1, \ldots, L), \quad p_{i_1} \cdot p_{i_2} \sim Q^2 \quad (i_1 \neq i_2).$$

small virtuality — large virtuality — wide-angle scattering

# *The "on–shell expansion"*

- We start with the following asymptotic expansion:

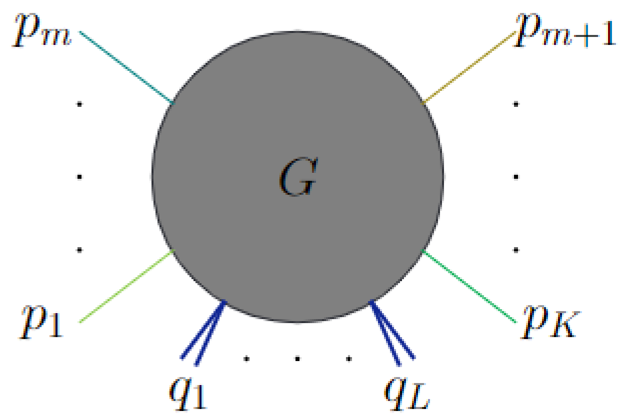


massless

$$p_i^2 \sim \lambda Q^2 \quad (i = 1, \ldots, K), \qquad q_j^2 \sim Q^2 \quad (j = 1, \ldots, L), \qquad p_{i_1} \cdot p_{i_2} \sim Q^2 \quad (i_1 \neq i_2).$$

small virtuality — large virtuality — wide-angle scattering

- ***Result: the possibly relevant modes are***

$$k_H^\mu \sim Q(1, 1, 1), \quad k_{C_i}^\mu \sim Q(1, \lambda, \lambda^{1/2}), \quad k_S^\mu \sim Q(\lambda, \lambda, \lambda).$$

# *Facet regions in the on–shell expansion*

- More precisely, the general structure of each facet region is

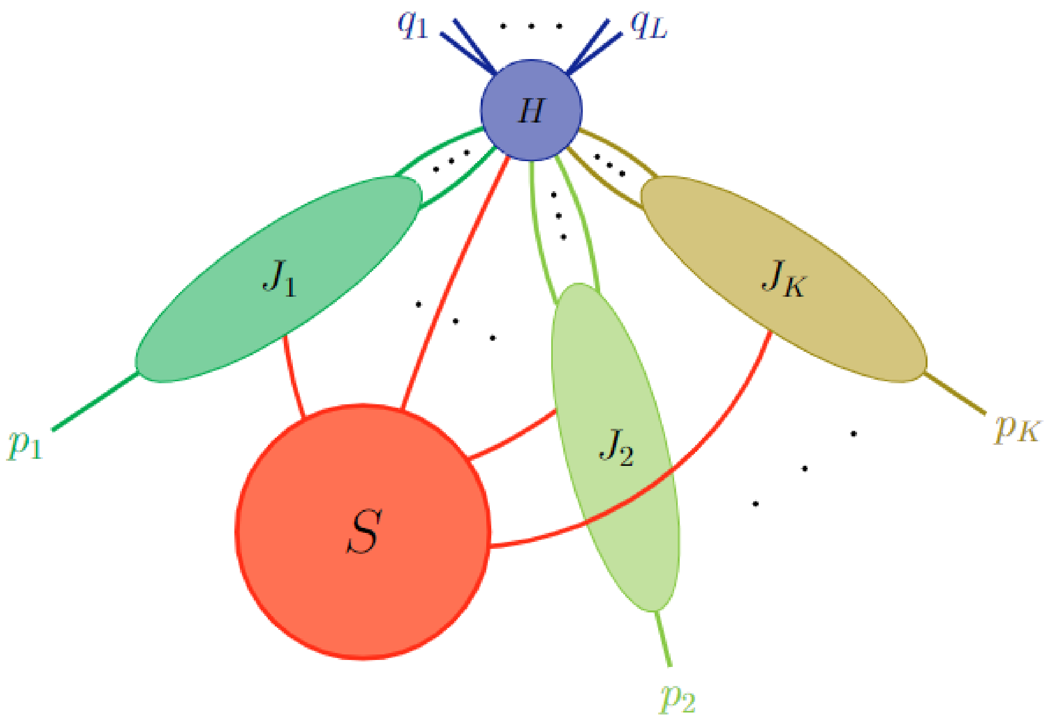


$$k_H^\mu \sim Q(1,1,1),$$

$$k_{C_i}^\mu \sim Q(1,\lambda,\lambda^{1/2}),$$

$$k_S^\mu \sim Q(\lambda,\lambda,\lambda).$$

with additional requirements on the subgraphs $H$, $J$, and $S$.

This conclusion was proposed in [E.Gardi, F.Herzog, S.Jones, YM, J.Schlenk, JHEP07(2023)197], and later proved in [YM, JHEP09(2024)197].

# *Some remarks*

1. There are additional requirements of the subgraphs $H, J,$ and $S$.

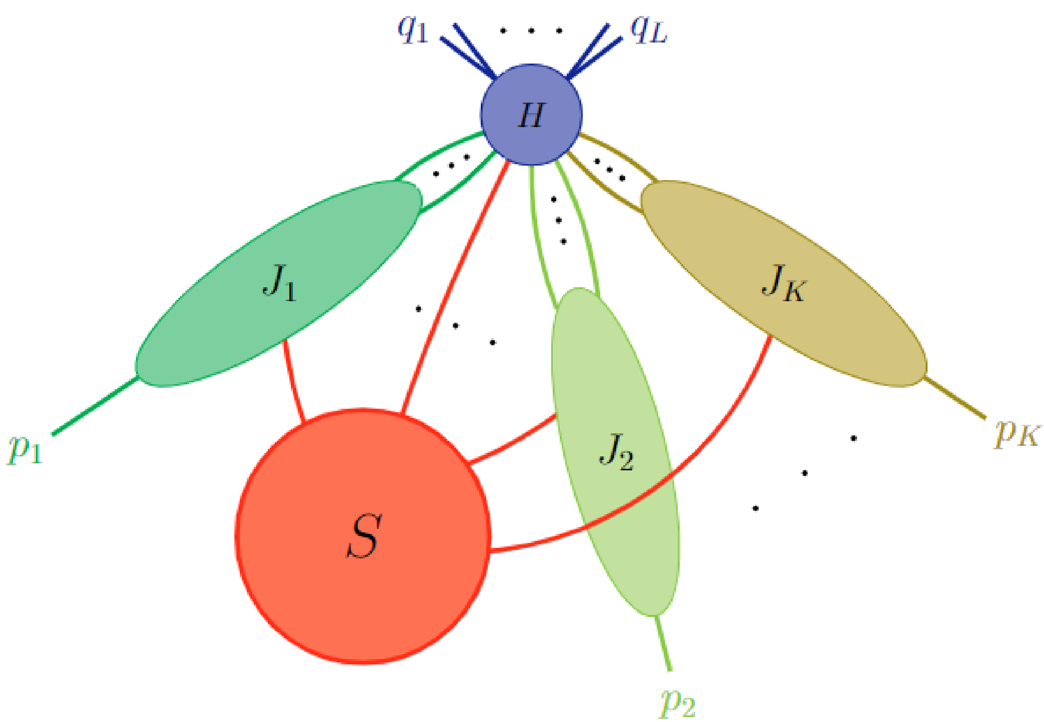


$$k_H^\mu \sim Q(1,1,1),$$

$$k_{C_i}^\mu \sim Q(1,\lambda,\lambda^{1/2}),$$

$$k_S^\mu \sim Q(\lambda,\lambda,\lambda).$$

For example, each connected component of $S$ attaches to ≥2 jets.

# Some remarks

2. <u>This picture is natural</u>

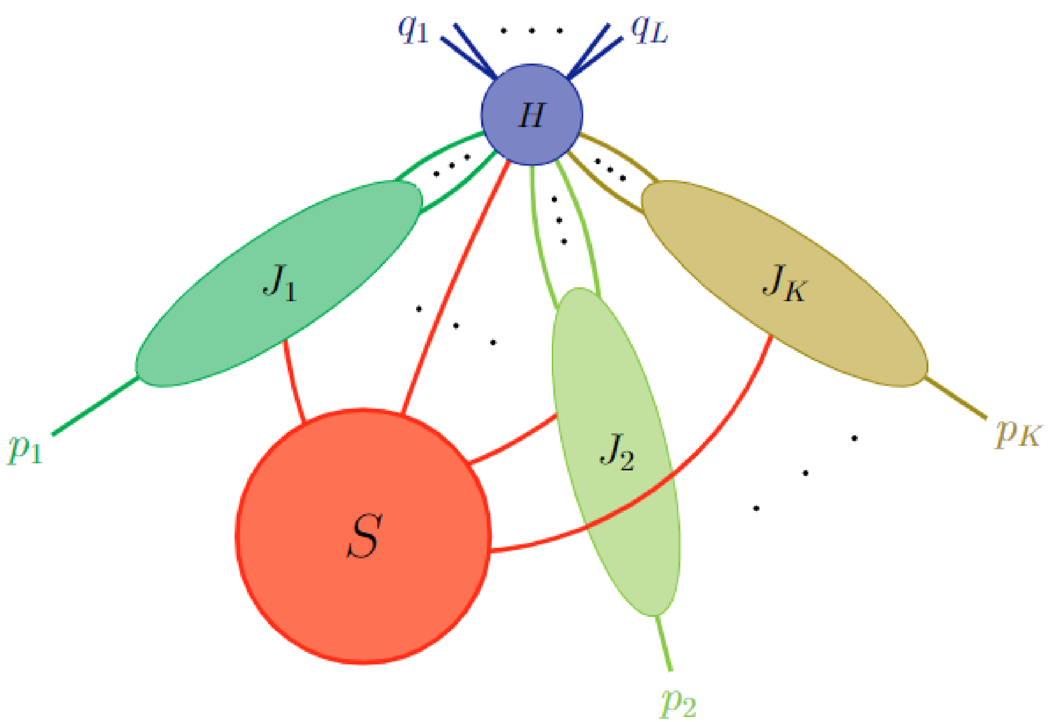


$$k_H^\mu \sim Q(1,1,1),$$

$$k_{C_i}^\mu \sim Q(1,\lambda,\lambda^{1/2}),$$

$$k_S^\mu \sim Q(\lambda,\lambda,\lambda).$$

because it is consistent with the "*pinch surfaces*", i.e., solutions of the Landau equations.

Landau equations characterize singularities of the Feynman integrand. Expansions should be made around these singularities.

# *Some remarks*

3. <u>This picture is highly nontrivial</u>

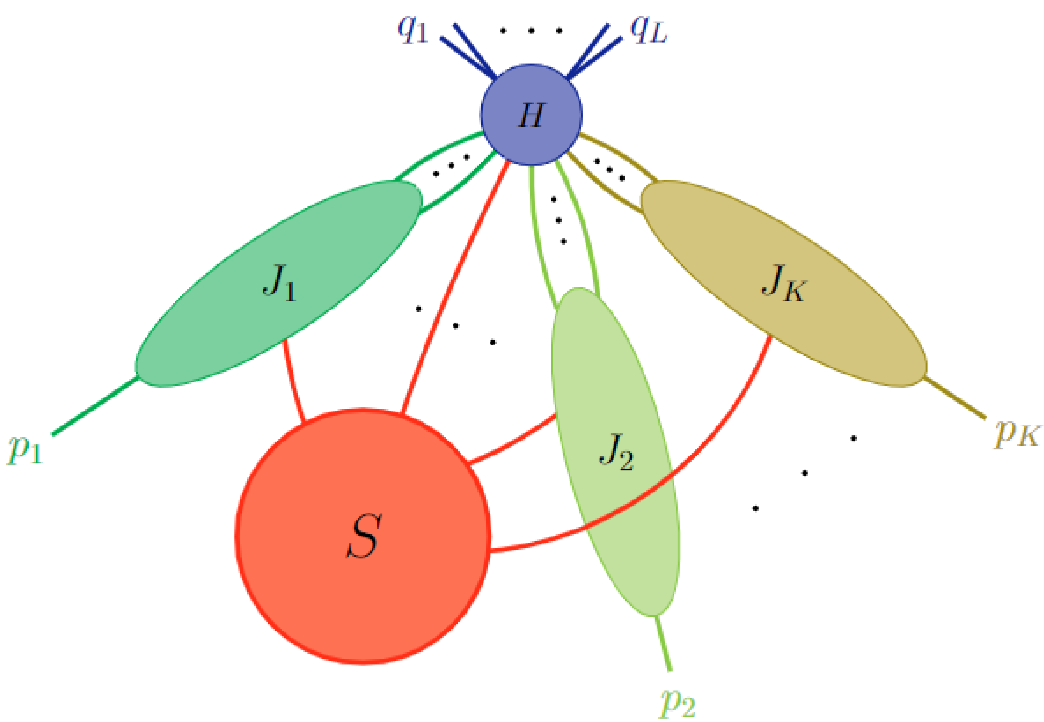


$$k_H^\mu \sim Q(1,1,1),$$

$$k_{C_i}^\mu \sim Q(1,\lambda,\lambda^{1/2}),$$

$$k_S^\mu \sim Q(\lambda,\lambda,\lambda).$$

because the small parameter λ is unique.

→ This further validates **SCETI** !

# *Phenomenology*

- Soft-Collinear Effective Theory (SCET): an effective theory describing the interactions of soft and collinear degrees of freedom in the presence of a hard interaction.
- For example, the SCET describing $e^+e^- \to \gamma^* \to \mathbf{dijets}$

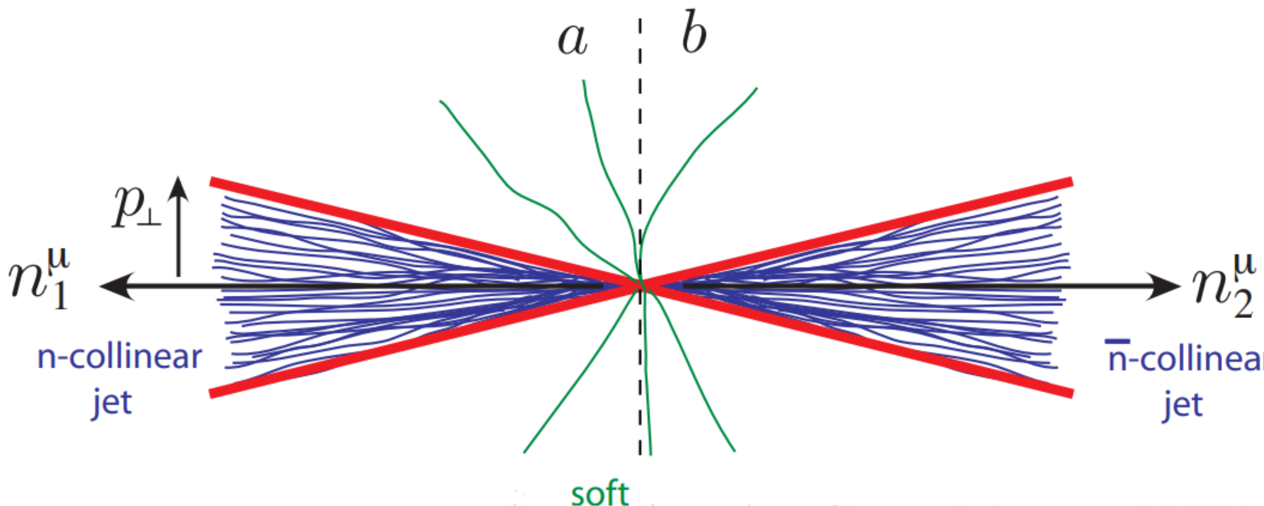


(Bauer & Stewart, SCET Lecture Notes 2013)

involves the hard mode (integrated out), the collinear modes, and the soft mode.

# Phenomenology

- Soft-Collinear Effective Theory (SCET): an effective theory describing the interactions of soft and collinear degrees of freedom in the presence of a hard interaction.
- The **SCET$_\mathrm{I}$ Lagrangian** (leading order):

$$\mathcal{L} = \sum_n (\mathcal{L}_{n\xi} + \mathcal{L}_{ng}) + \mathcal{L}_{\rm soft}$$

$$= \sum_n \Bigg( e^{-ix\cdot\mathcal{P}} \bar{\xi}_n \left( in\cdot D + i\not{D}_{n\perp} \frac{1}{i\bar{n}\cdot D_n} \not{D}_{n\perp} \right) \frac{\not{\bar{n}}}{2} \xi_n$$

$$+ \frac{1}{2g^2} \mathrm{Tr}\{[i\mathcal{D}^\mu, i\mathcal{D}_\mu]^2\} + \tau \mathrm{Tr}\{[i\mathcal{D}_{\rm s}^\mu, A_{n\mu}]^2\} + 2\mathrm{Tr}\{b_n [i\mathcal{D}_{\rm s}^\mu, [i\mathcal{D}_\mu, c_n]]\} \Bigg)$$

$$+ \bar{\psi}_{\rm s} i\not{D}_{\rm s} \psi_{\rm s} - \frac{1}{2} \mathrm{Tr}\{G_{\rm s}^{\mu\nu} G_{{\rm s},\mu\nu}\} + \tau_{\rm s} \mathrm{Tr}\{(i\partial_\mu A_{\rm s}^\mu)^2\} + 2\mathrm{Tr}\{b_{\rm s} i\partial_\mu i\mathcal{D}_{\rm s}^\mu c_{\rm s}\}\,.$$

- ***We have shown that, in the regime of the on–shell expansion, nothing can go beyond the prediction of SCET, as long as all the regions are predicted by lower facets.***

# *Some remarks*

4. Note that this picture is different from the "leading pinch surfaces".

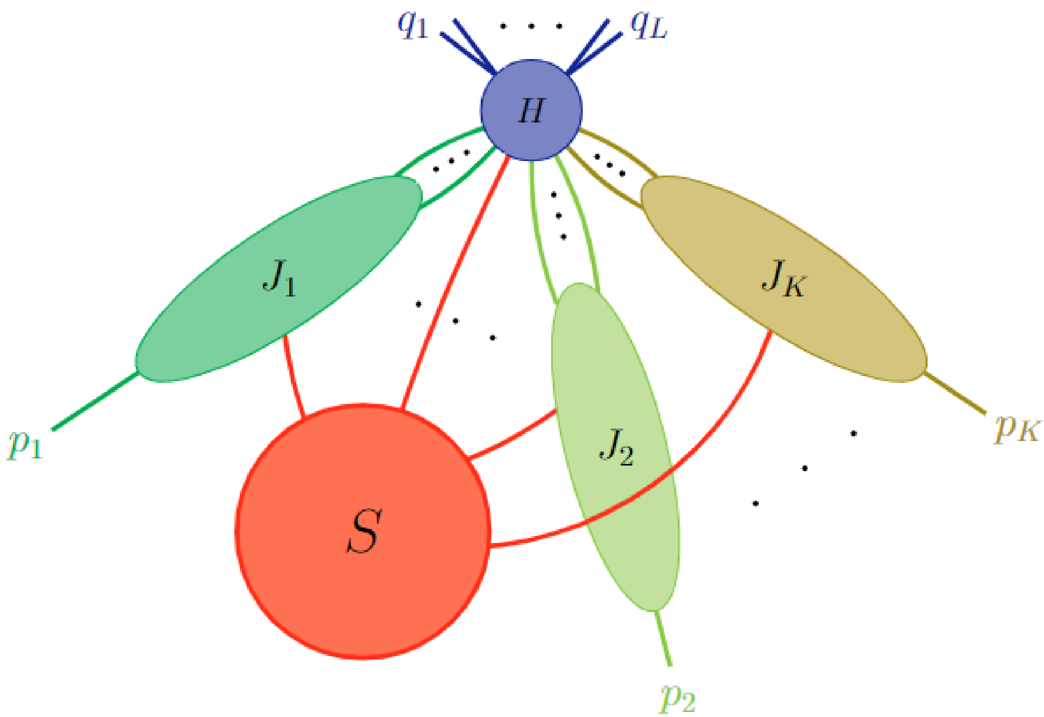


$$k_H^\mu \sim Q(1, 1, 1),$$

$$k_{C_i}^\mu \sim Q(1, \lambda, \lambda^{1/2}),$$

$$k_S^\mu \sim Q(\lambda, \lambda, \lambda).$$

Leading pinch surfaces: those contributing to the infrared divergences in gauge theory. Further requirements of $H, J$, and $S$ are needed as a result of power counting.

For example, $S$ cannot attach to $H$ directly.

# *Hidden regions in the on–shell expansion*

- Most of the regions are facet regions:
  - most graphs have only facet regions;
  - for the remaining graphs, hidden regions are very few compared with the facet regions.

- For the 2->2 massless wide-angle scattering graphs,
  - one loop: no graphs with hidden regions;
  - two loops: ≈100 graphs, none with hidden regions;
  - three loops: ≈1000 graphs, 10 of them have hidden regions.

# *Hidden regions in the on–shell expansion*

- Most of the regions are facet regions:
  - most graphs have only facet regions;
  - for the remaining graphs, hidden regions are very few compared with the facet regions.

- For the 2->2 massless wide-angle scattering graphs,
  - one loop: no graphs with hidden regions;
  - two loops: ≈100 graphs, none with hidden regions;
  - three loops: ≈1000 graphs, 10 of them have hidden regions.

same origin

only 1 for each graph; "Landshoff scattering"

# *Hidden regions in the on–shell expansion*

- The "*Landshoff scattering*":

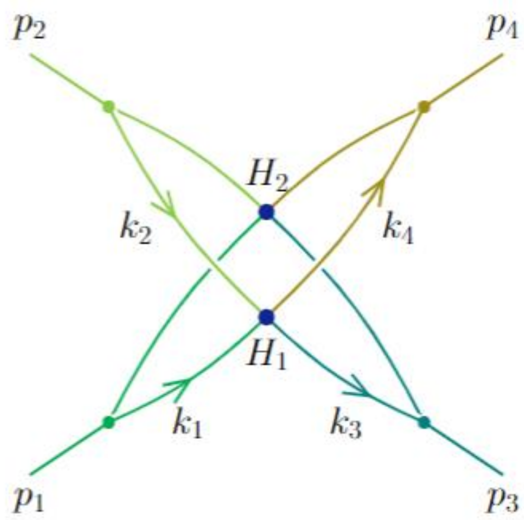


- In scalar theory, from straightforward power counting, above is **the only** region that contributes to the leading asymptotic behavior. So this region must be included.
- This region **cannot** be detected by any computer codes.

E.Gardi, F.Herzog, S.Jones, YM, JHEP08(2024)127

# *Power counting details*

- To see why this region is leading:

$$k_i^\mu = Q\left(\xi_i v_i^\mu + \lambda\kappa_i\bar{v}_i^\mu + \sqrt{\lambda}\tau_i u_i^\mu + \sqrt{\lambda}\nu_i n^\mu\right), \qquad i = 1,2,3,4.$$

(Botts & Sterman, 1989)

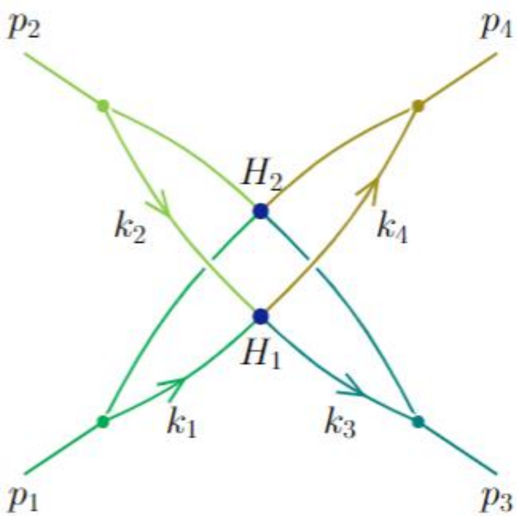


$$\xi_2 = \xi_1 - \frac{1}{2}\sqrt{\lambda}\cos^2(\theta)\left(\tan\left(\frac{\theta}{2}\right)\Delta\tau - \cot\left(\frac{\theta}{2}\right)\Sigma\tau\right) + \lambda(\kappa_2 - \kappa_1),$$

$$\xi_3 = \xi_1 + \frac{1}{2}\sqrt{\lambda}\tan\left(\frac{\theta}{2}\right)\Delta\tau + \lambda(\kappa_2 - \kappa_4),$$

$$\xi_4 = \xi_1 - \frac{1}{2}\sqrt{\lambda}\cot\left(\frac{\theta}{2}\right)\Sigma\tau + \lambda(\kappa_2 - \kappa_3).$$

- With this parameterization, $\int d^D k_1 d^D k_2 d^D k_3 = Q^{3D}\int\prod_{i=1}^{3} d\xi_i d\kappa_i d\tau_i d\nu_i$

- Under change of variables $\{\xi_2, \xi_3\} \to \{\kappa_4, \tau_4\}$,

$$\det\left(\frac{\partial(\xi_2,\xi_3)}{\partial(\kappa_4,\tau_4)}\right) = \lambda^{3/2}\cos(\theta)\cot(\theta)\,.$$

E.Gardi, F.Herzog, S.Jones, YM, JHEP08(2024)127

# *Power counting details*

- To see why this region is leading:

$$k_i^\mu = Q\left(\xi_i v_i^\mu + \lambda\kappa_i \bar{v}_i^\mu + \sqrt{\lambda}\tau_i u_i^\mu + \sqrt{\lambda}\nu_i n^\mu\right), \qquad i = 1, 2, 3, 4.$$

(Botts & Sterman, 1989)

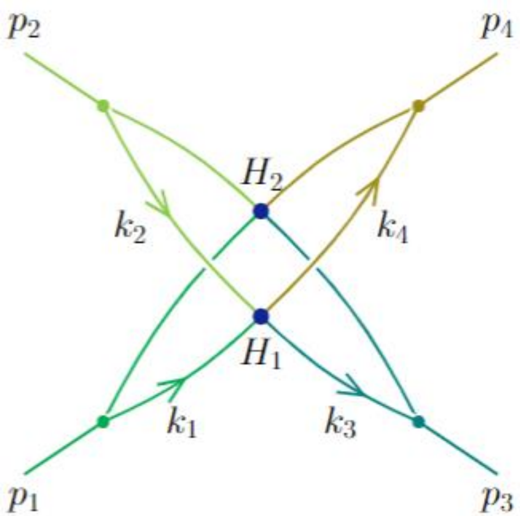


$$\int \prod_{i=1}^{3} d\xi_i\, d\kappa_i d\tau_i d\nu_i = \mathcal{C}\cdot \int_0^1 d\xi_1 \underbrace{\left(\int \prod_{i=1}^{3} (\lambda d\kappa_i)(\lambda^{\frac{1}{2}} d\tau_i)(\lambda^{\frac{1}{2}} d\nu_i)^{1-2\epsilon}\right)}_{\lambda^{6-3\epsilon}}$$

$$\cdot \int d\kappa_4 d\tau_4\, \underbrace{\det\left(\frac{\partial(\xi_2,\xi_3)}{\partial(\kappa_4,\tau_4)}\right)}_{\lambda^{3/2}}\,.$$

- Power counting result:

$$\mathcal{I} \sim \lambda^\mu, \qquad \mu = -\frac{1}{2} - 3\epsilon.$$

- Meanwhile, **μ ≥ 0** for all the other regions.

E.Gardi, F.Herzog, S.Jones, YM, JHEP08(2024)127

# Numerical evidences

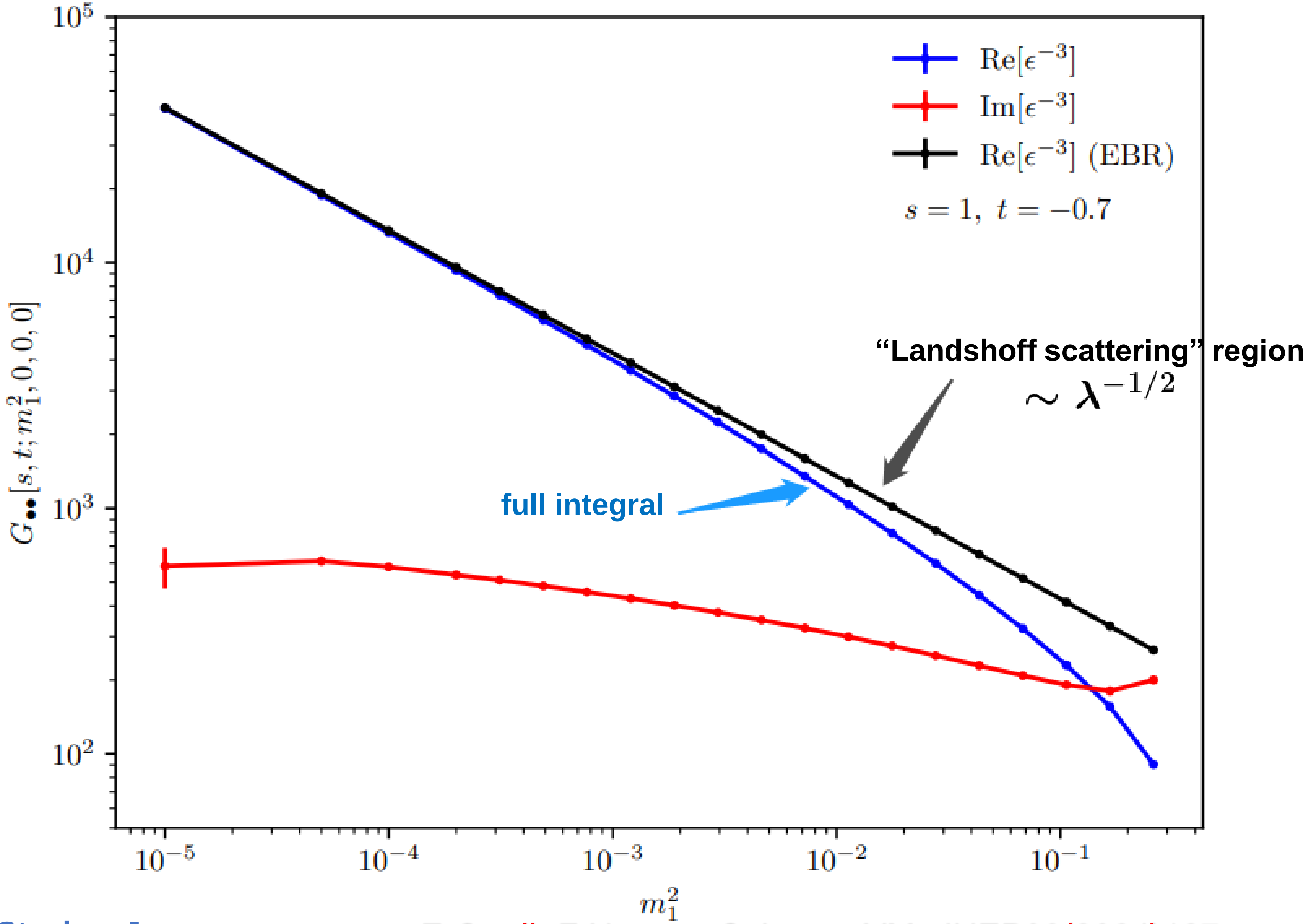


Graph by Stephen Jones

E.Gardi, F.Herzog, S.Jones, YM, JHEP08(2024)127

# *Numerical evidences*

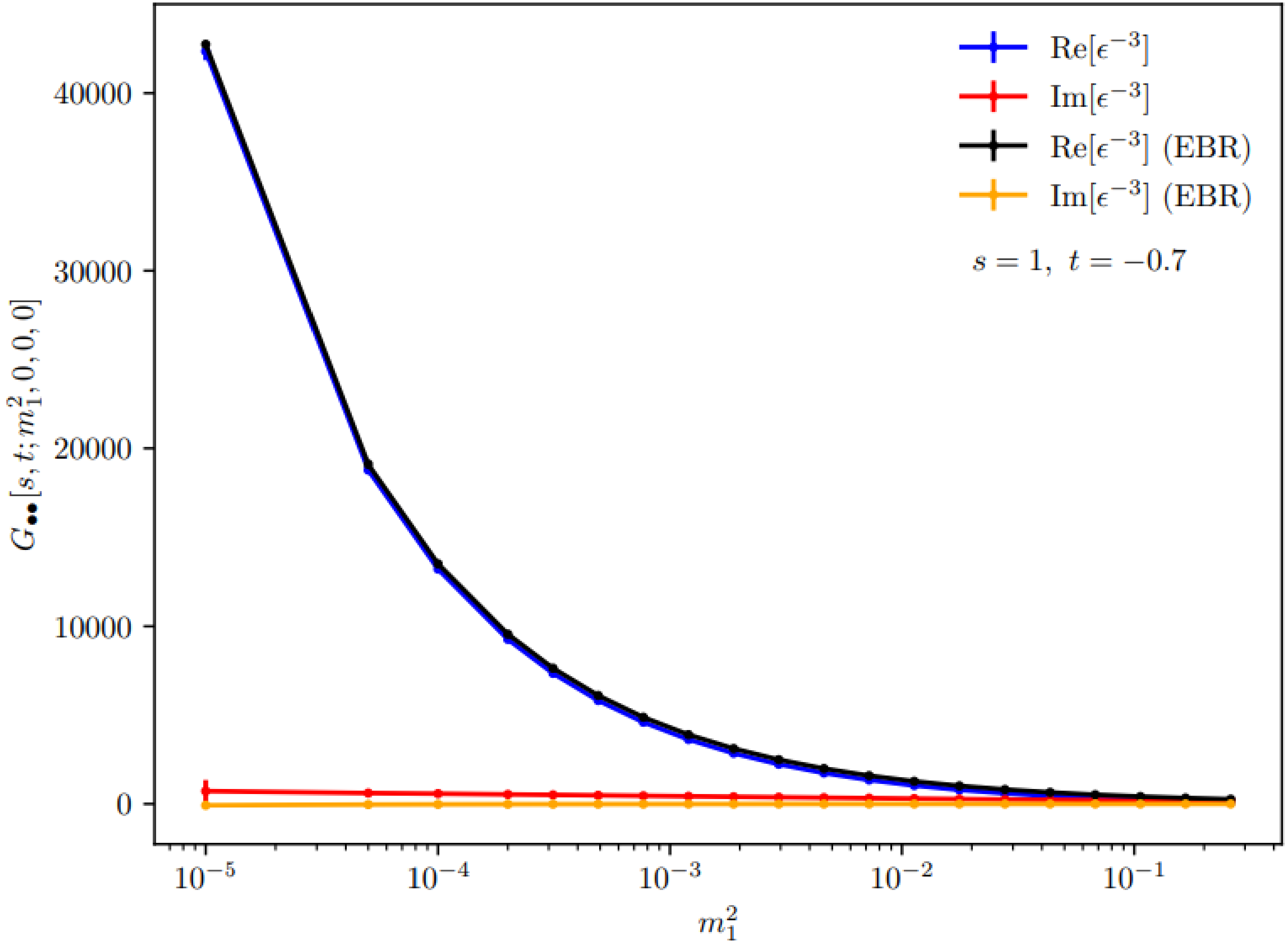


Graph by Stephen Jones

E.Gardi, F.Herzog, S.Jones, YM, JHEP08(2024)127

# *The whole list of subtle graphs*

- All the 3-loop graphs

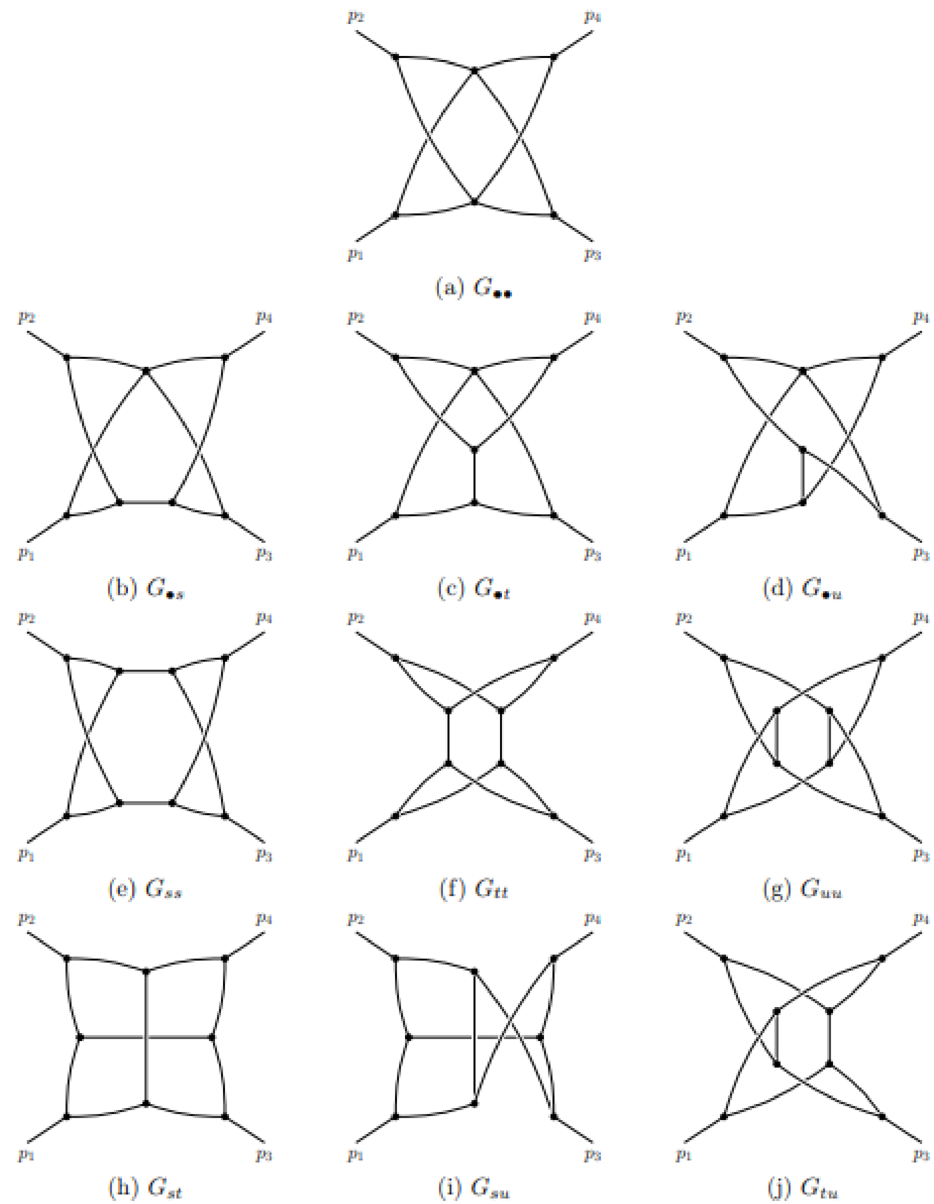

# *The whole list of subtle graphs*

- Corresponding regions

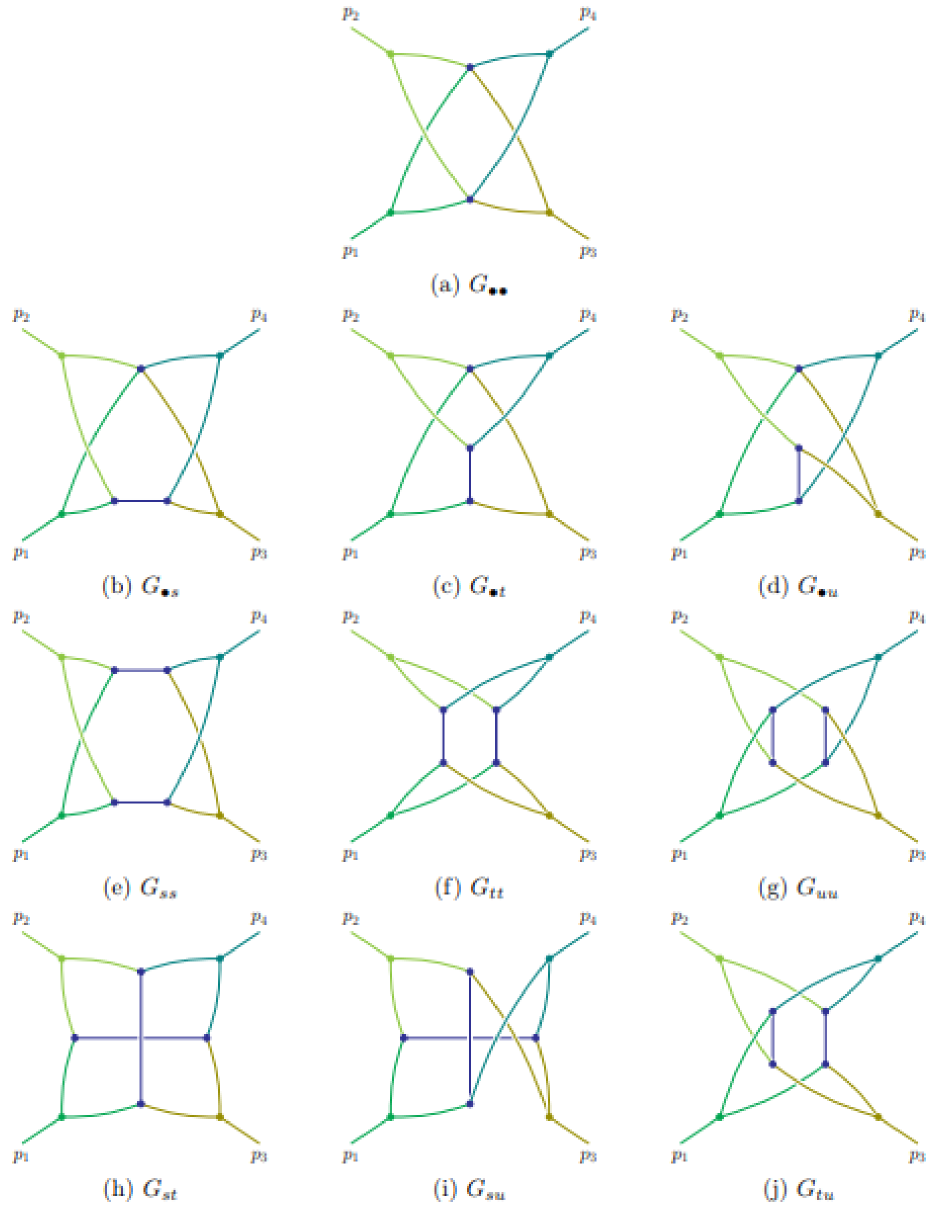

# *The whole list of subtle graphs*

- Corresponding regions

<u>*To identify these regions*</u>:

***Dissect*** *the original polytope into several distinct sectors, such that these regions, which are hidden inside the original polytope, appear as lower facets of the new sub-polytopes.*

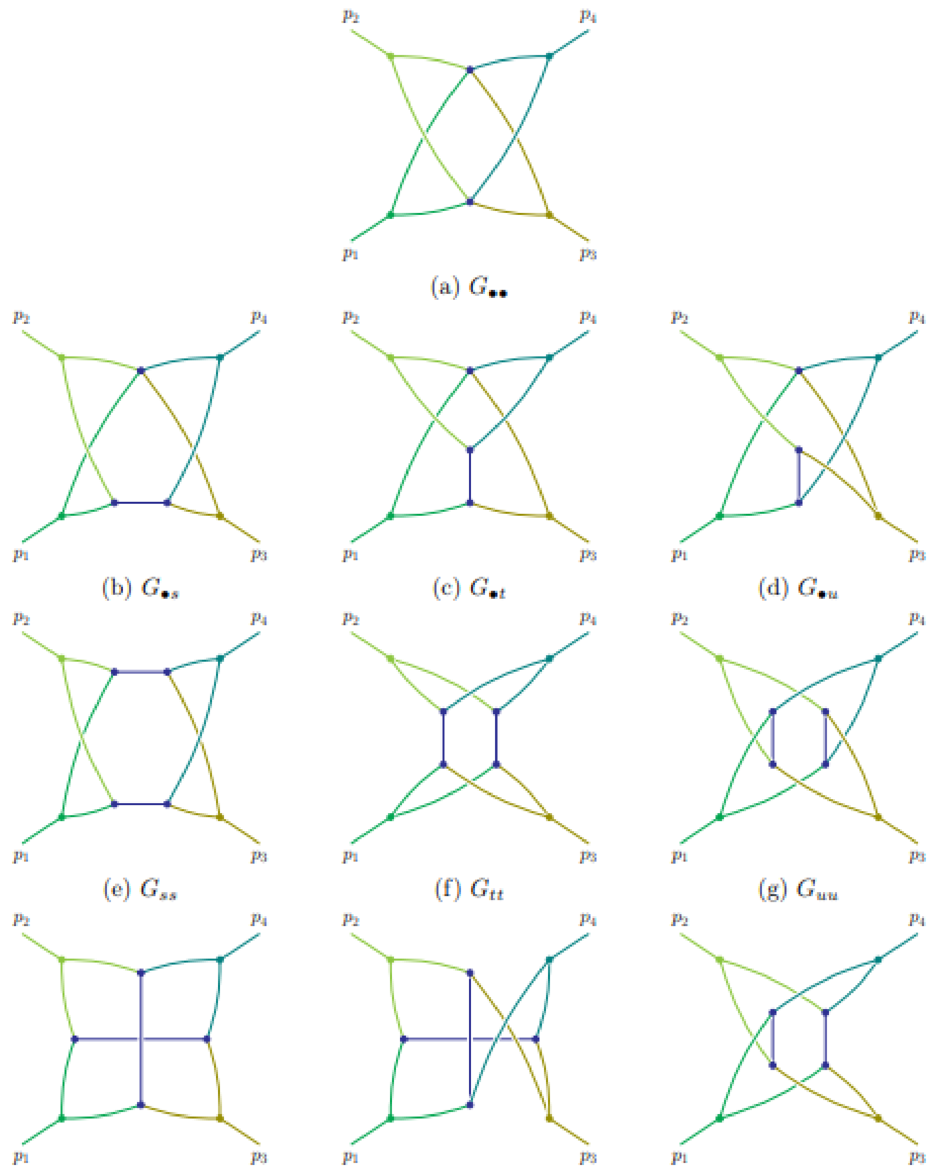


(a) $G_{\bullet\bullet}$ (b) $G_{\bullet s}$ (c) $G_{\bullet t}$ (d) $G_{\bullet u}$ (e) $G_{ss}$ (f) $G_{tt}$ (g) $G_{uu}$ (h) $G_{st}$ (i) $G_{su}$ (j) $G_{tu}$

# *Regions in the on–shell expansion*

***Conjecture:***

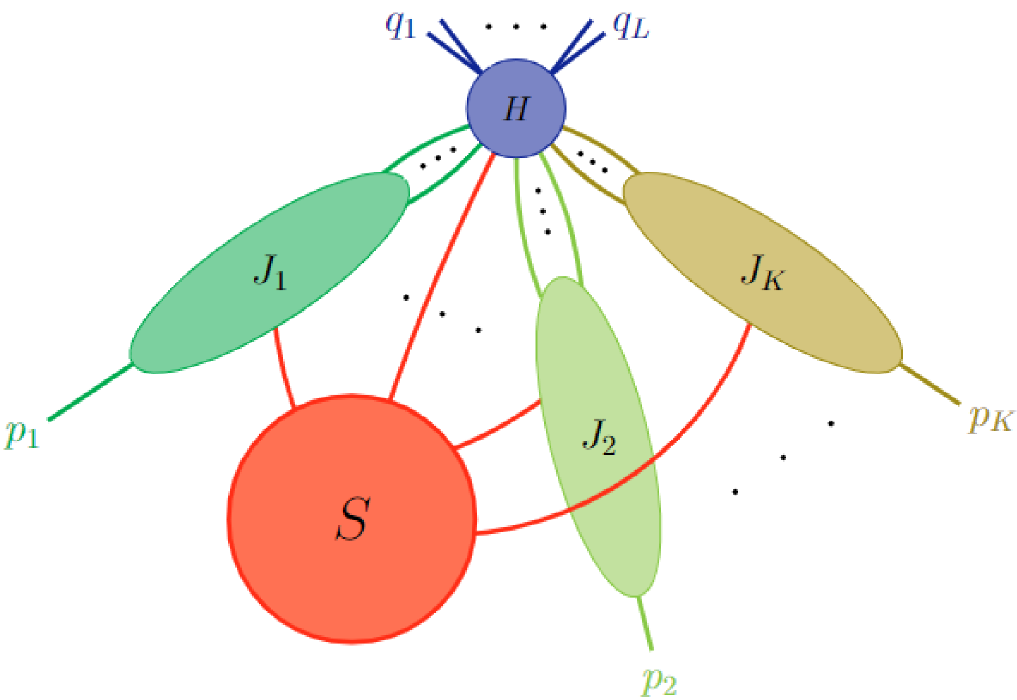


**facet region**

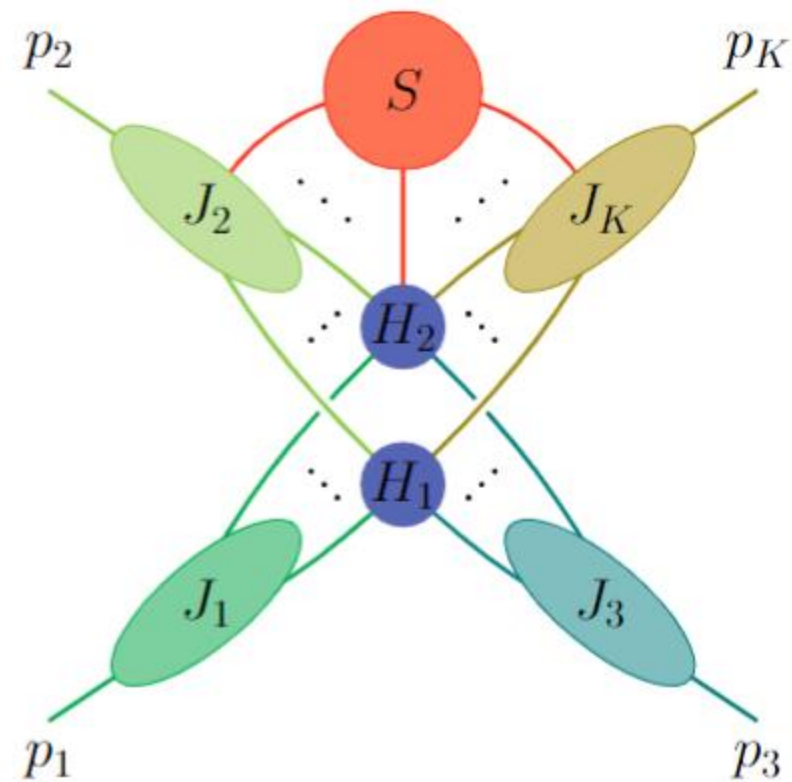


**hidden region**

E.Gardi, F.Herzog, S.Jones, YM, JHEP08(2024)127

# How about other expansions?

# *The "soft expansion"*

- Including some soft external momenta

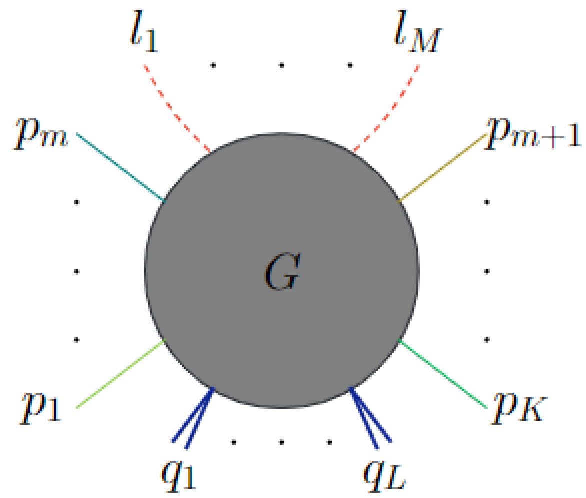


**massless**

**exactly on-shell** **large virtuality** **exactly on-shell**

$$p_i^2 = 0 \quad (i=1,\dots,K), \quad q_j^2 \sim Q^2 \quad (j=1,\dots,L), \quad l_k^2 = 0 \quad (k=1,\dots,M),$$
$$p_{i_1}\cdot p_{i_2} \sim Q^2 \quad (i_1 \neq i_2), \quad p_i \cdot l_k \sim q_j \cdot l_k \sim \lambda Q^2, \quad l_{k_1}\cdot l_{k_2} \sim \lambda^2 Q^2 \quad (k_1 \neq k_2).$$

**wide-angle scattering** **soft momenta**

YM, JHEP09(2024)197

# Regions in the soft expansion

- ***Result: the possibly relevant modes are:***

$$k_H^\mu \sim Q(1,1,1), \quad k_{C_i}^\mu \sim Q(1,\lambda,\lambda^{1/2}), \quad k_S^\mu \sim Q(\lambda,\lambda,\lambda).$$

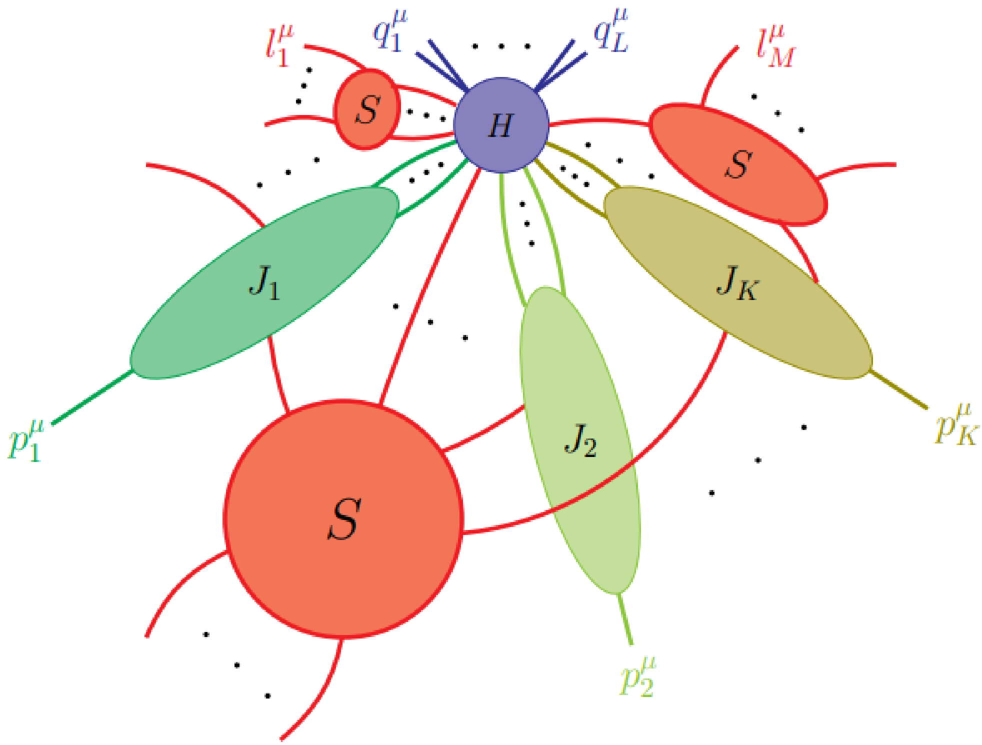


- Interesting feature: additional requirements for the subgraphs.

YM, JHEP09(2024)197

# *Regions in the soft expansion*

- The interactions between the soft subgraph and the jets follow the "infection-spreading" picture.
- Each jet must be "infected" by some soft external momenta.
- Any soft component adjacent to ≥3 jets can "spread the infection".
- Example:

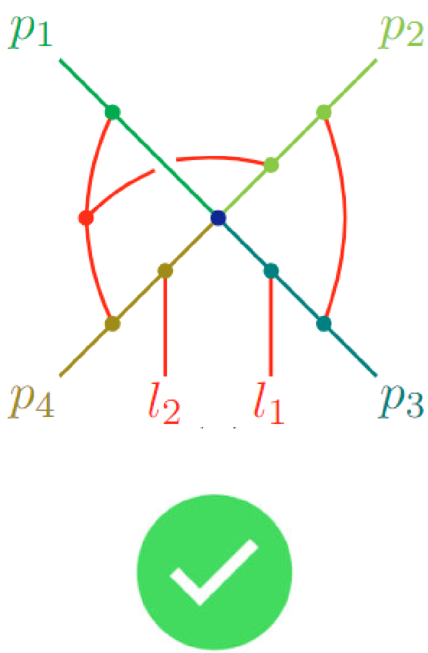


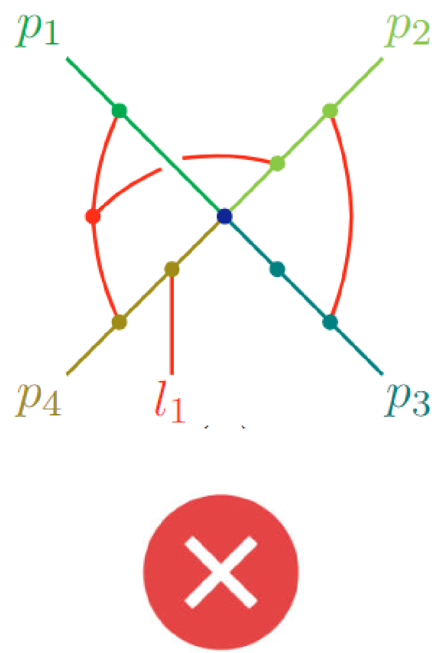


YM, JHEP09(2024)197

# *Regions in the soft expansion*

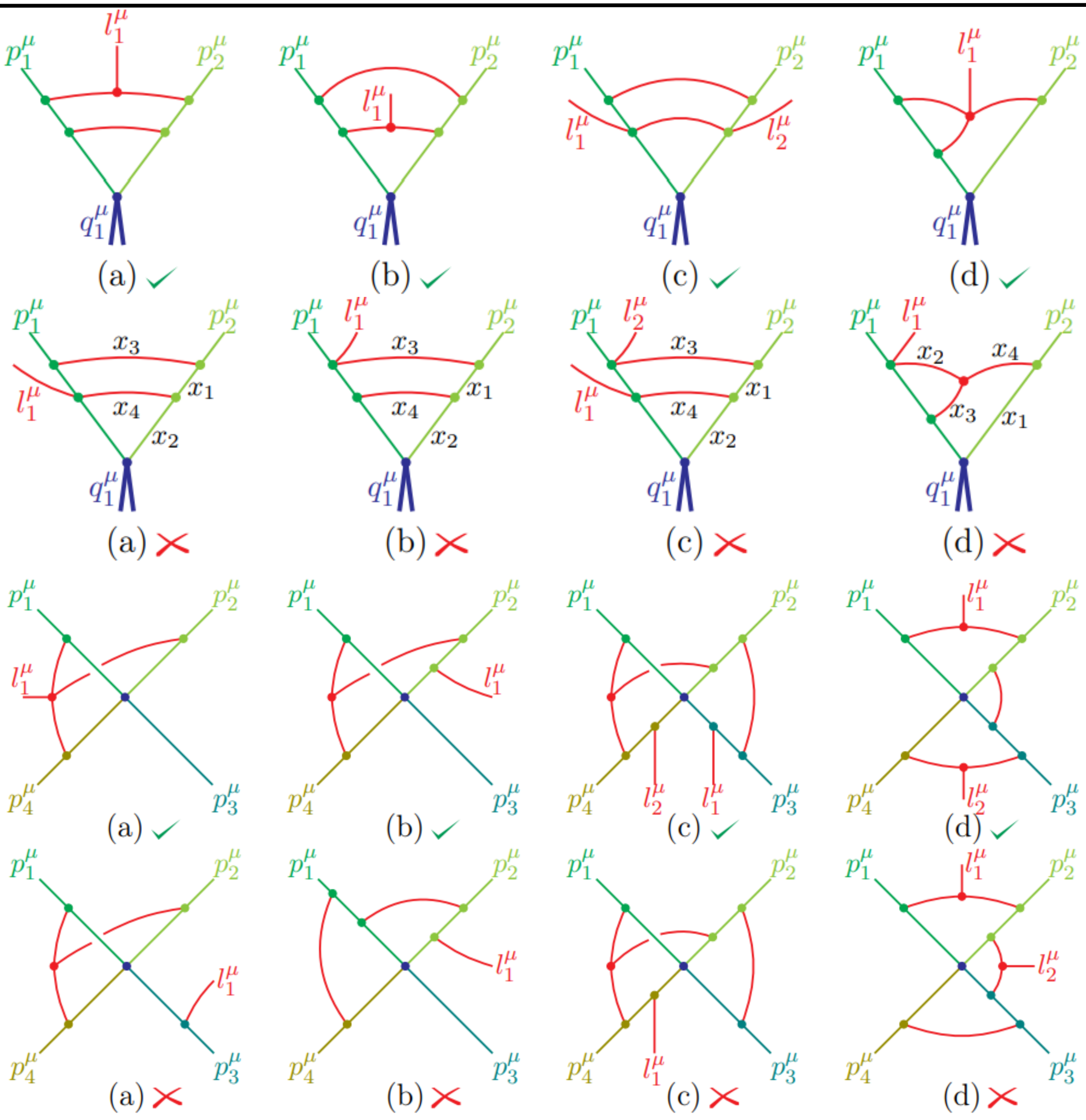


YM, JHEP09(2024)197

# *Regions in the soft expansion*

- This study may also go beyond QCD.
- For example, some rules for the "Soft-Collinear Gravity" coincide with what we have found:

graviton attached to a purely soft vertex.

The above argument generalises to the following all-order statement: *In soft loop-corrections to the soft theorem, contrary to the tree-level case, the emitted soft graviton must always attach to a purely-soft vertex, and never directly to any of the energetic particle lines.* The reason is that soft-collinear interactions involve the soft field at the multipole-expanded point $x_-^\mu$ to any order in the $\lambda$-expansion. Hence, if the emitted graviton couples directly to an energetic line, one can always route its momentum such that the entire loop integral will depend only on $n_{i-}k n_{i+}^\mu/2$ of a single collinear direction, $i$, and no soft invariant can be formed to provide a scale to the loop diagram.

Continuing with two soft loops, whenever the diagram contains a second purely

(Beneke, Hager, Szafron, "*Soft-Collinear Gravity and Soft Theorems*")
See also
(Beneke, Hager, Szafron, 2021)
(Beneke, Hager, Schwienbacher, 2022)
(Beneke, Hager, Sanfilippo, 2023) et al.

# *The “mass expansion”*

- The heavy-to-light decay process:

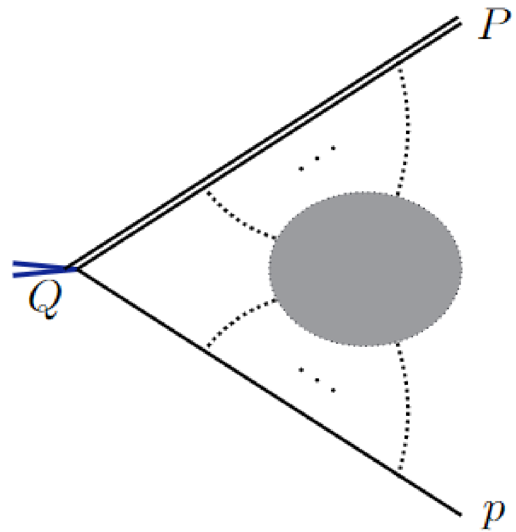


$$P^2 = M^2 \sim Q^2, \quad p^2 = m^2 \sim \lambda Q^2, \quad P \cdot p \sim Q^2.$$

**large mass** **small mass**

- In addition to the hard, collinear, and soft modes, more complicated modes can be present.

YM, JHEP09(2024)197

# *Regions in the mass expansion*

- More modes are included:

| | Starting from |
|---|---|
| hard mode Q(1,1,1), | 1 loop |
| collinear mode $Q(1,\lambda,\lambda^{½})$, | 1 loop |
| soft mode $Q(\lambda,\lambda,\lambda)$, | 2 loops |
| soft·collinear mode $Q(\lambda,\lambda^2,\lambda^{3/2})$, | 3 loops |
| soft$^2$ mode $Q(\lambda^2,\lambda^2,\lambda^2)$, …. | 4 loops |
| semihard mode $Q(\lambda^{½},\lambda^{½},\lambda^{½})$, | 2 loops |
| semihard·collinear, semihard·soft, …., | 3 loops, nonplanar |
| semicollinear mode $Q(1,\lambda^{1/2},\lambda^{1/4})$, | 3 loops, nonplanar |
| semihard·semicollinear, …. | 4 loops, nonplanar |

YM, JHEP09(2024)197

# *Regions in the mass expansion*

- Examples

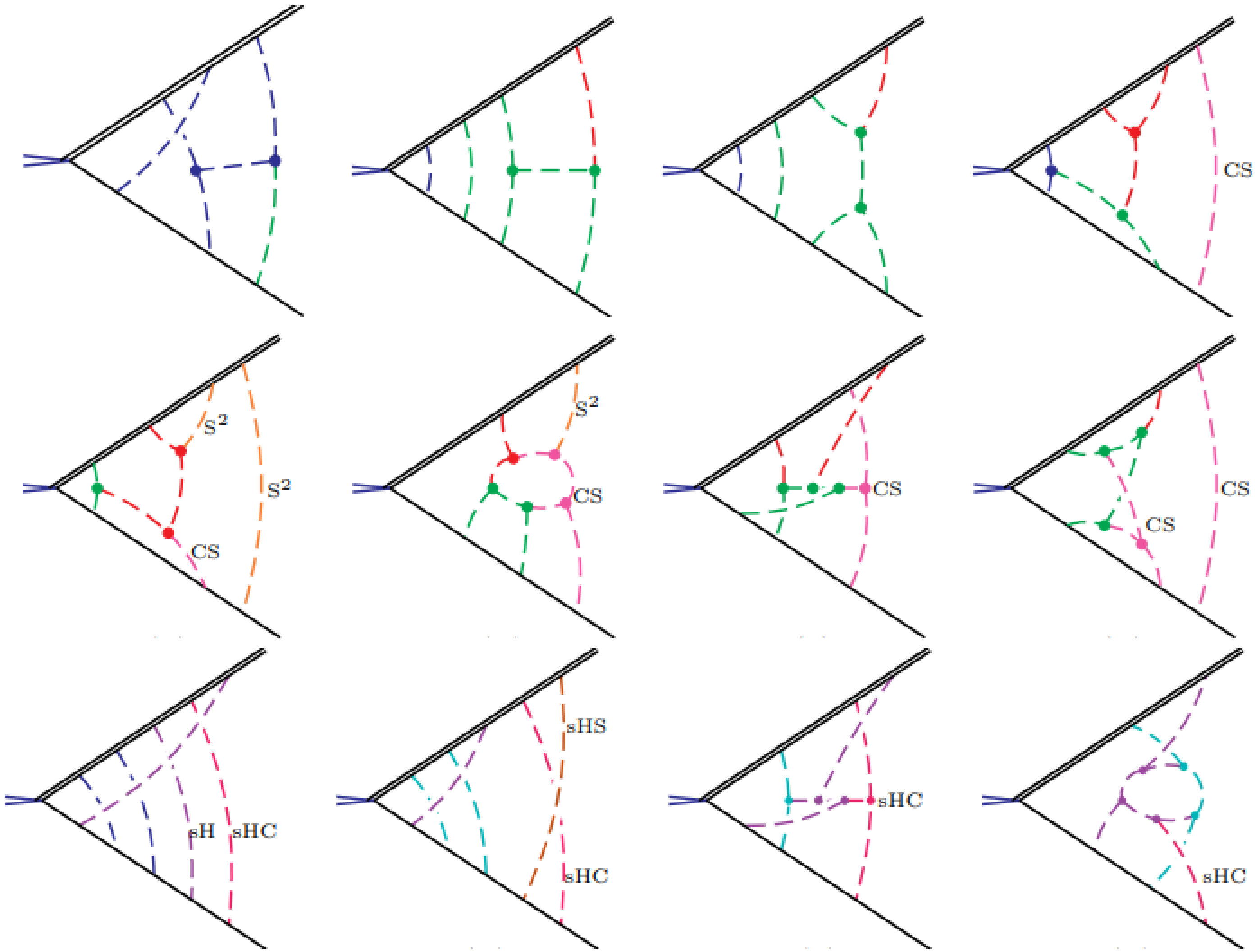

# A formalism for planar graphs

- For planar graphs, each region can be depicted as a "***terrace***".

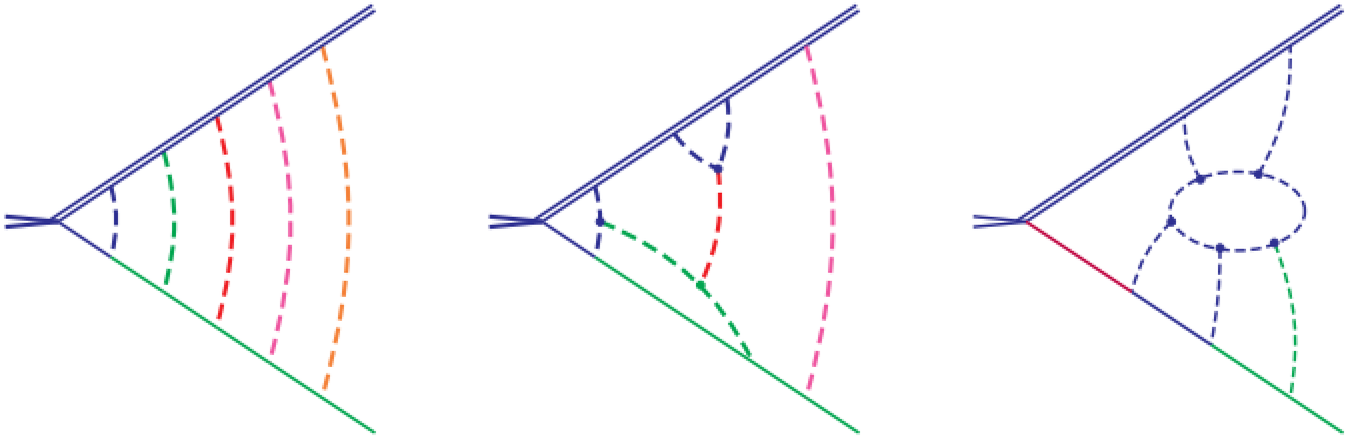

(a) (b) (c)

YM, JHEP09(2024)197

# A formalism for planar graphs

- For planar graphs, each region can be depicted as a "***terrace***".

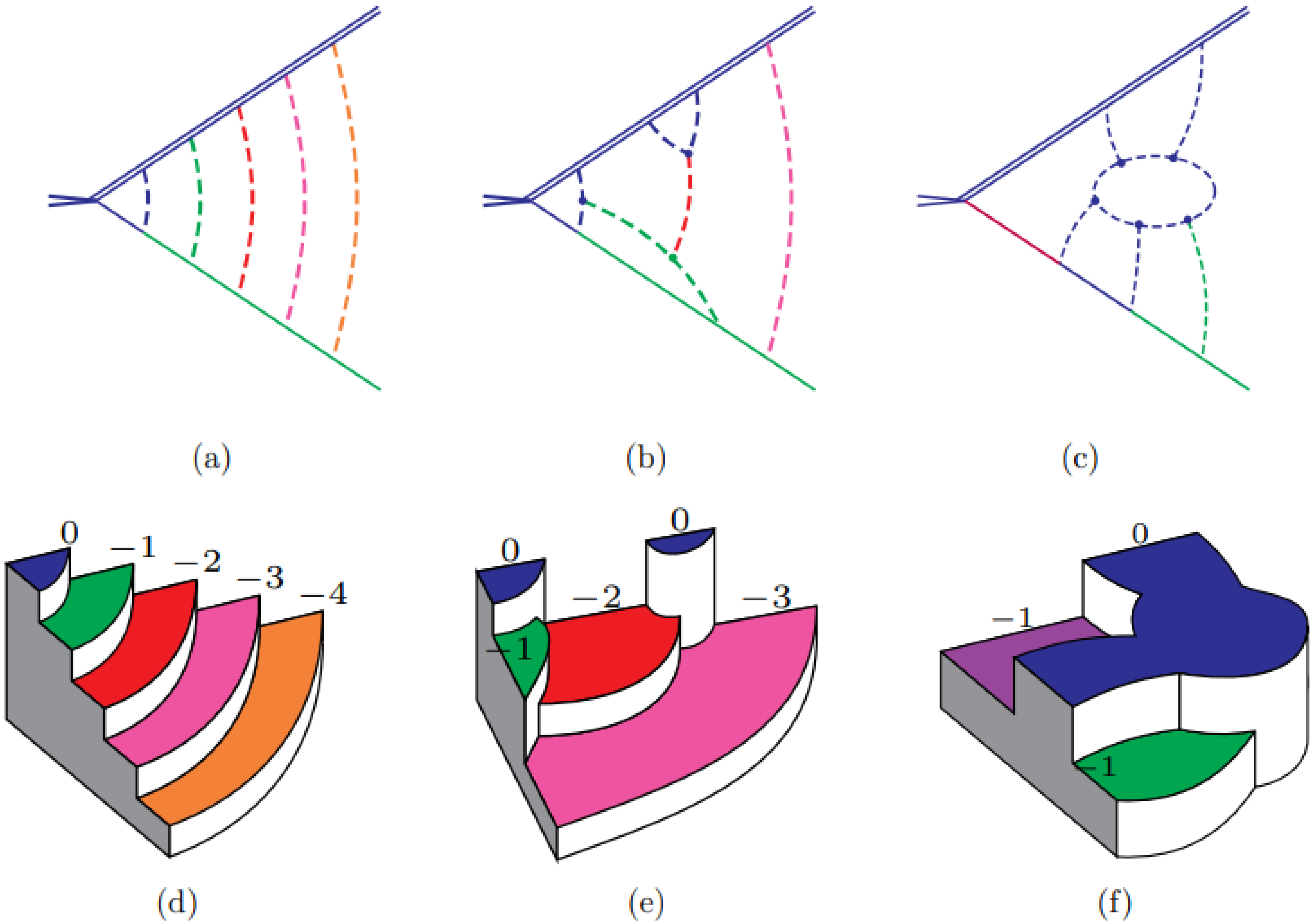


YM, JHEP09(2024)197

# *A formalism for planar graphs*

- For planar graphs, each region can be depicted as a "***terrace***".

(d) (e) (f)

YM, JHEP09(2024)197

# *High–energy expansion of forward scattering*

Consider the Regge limit of the 2-to-2 forward scattering.

Regions include:

hard, collinear, soft, *Glauber*, soft·collinear, collinear$^3$, …

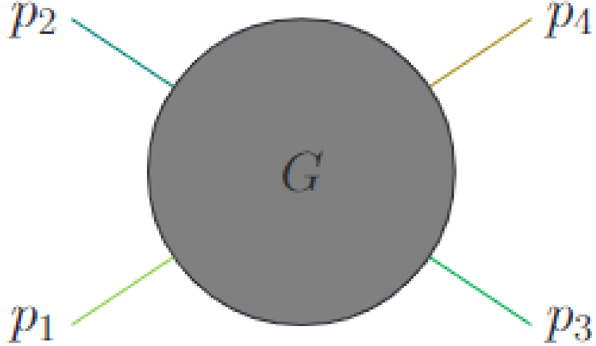


$$(p_1+p_2)^2 = s,$$
$$(p_1+p_3)^2 = t,$$
$$(p_1+p_4)^2 = u,$$

kinematic limit:

$$p_1^2 = p_2^2 = p_3^2 = p_4^2 = 0,$$
$$|t| \ll s \sim |u|,$$

E.Gardi, F.Herzog, S.Jones, YM, JHEP08(2024)127

# *High–energy expansion of forward scattering*

Consider the Regge limit of the 2-to-2 forward scattering.

Regions include:

hard, collinear, soft, *Glauber*, soft·collinear, collinear$^3$, …

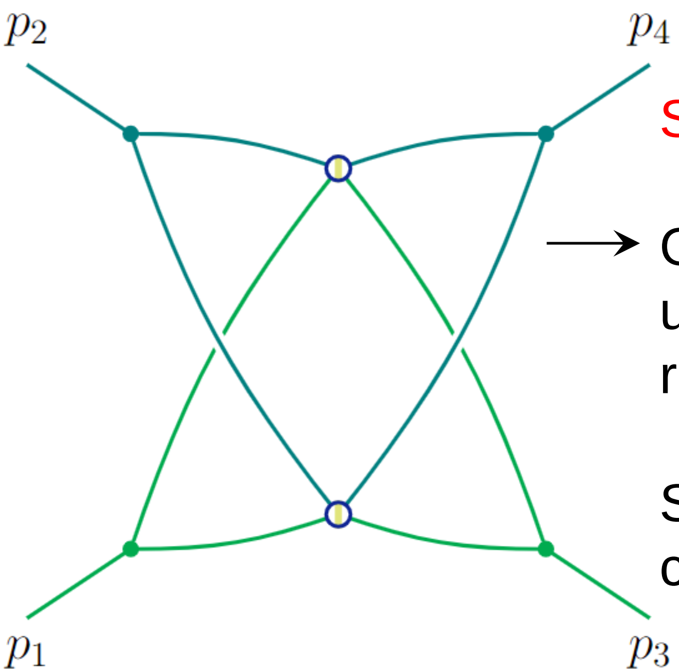


Scaling $(\lambda, \lambda, \lambda^{1/2})$, occurring from 3 loops.

→ Glauber momentum exchange between the upper and lower jets is a feature of hidden regions.

Such hidden regions cannot be detected by any computer codes.

E.Gardi, F.Herzog, S.Jones, YM, JHEP08(2024)127

# *High–energy expansion of forward scattering*

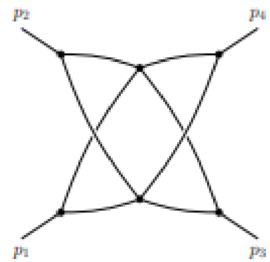


(a) $G_{\bullet\bullet}$

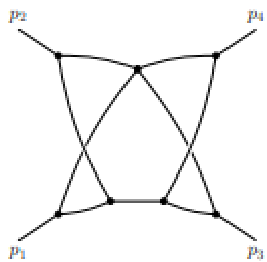


(b) $G_{\bullet s}$

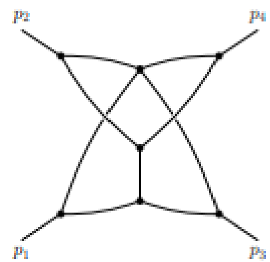


(c) $G_{\bullet t}$

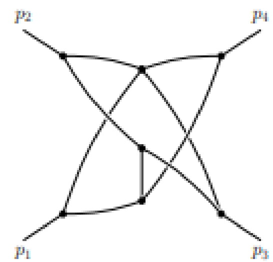


(d) $G_{\bullet u}$

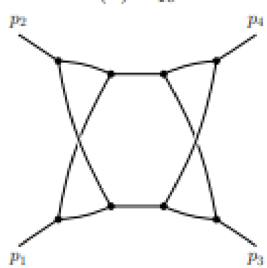


(e) $G_{ss}$

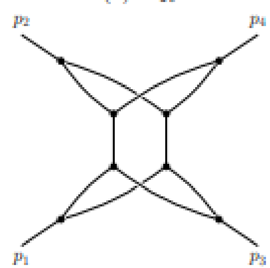


(f) $G_{tt}$

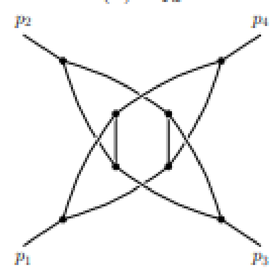


(g) $G_{uu}$

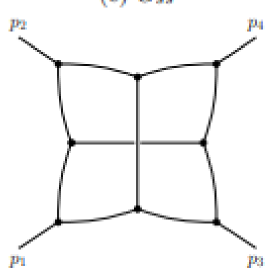


(h) $G_{st}$

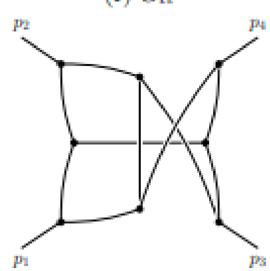


(i) $G_{su}$

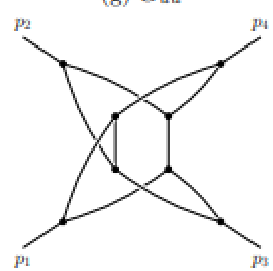


(j) $G_{tu}$

# *High–energy expansion of forward scattering*

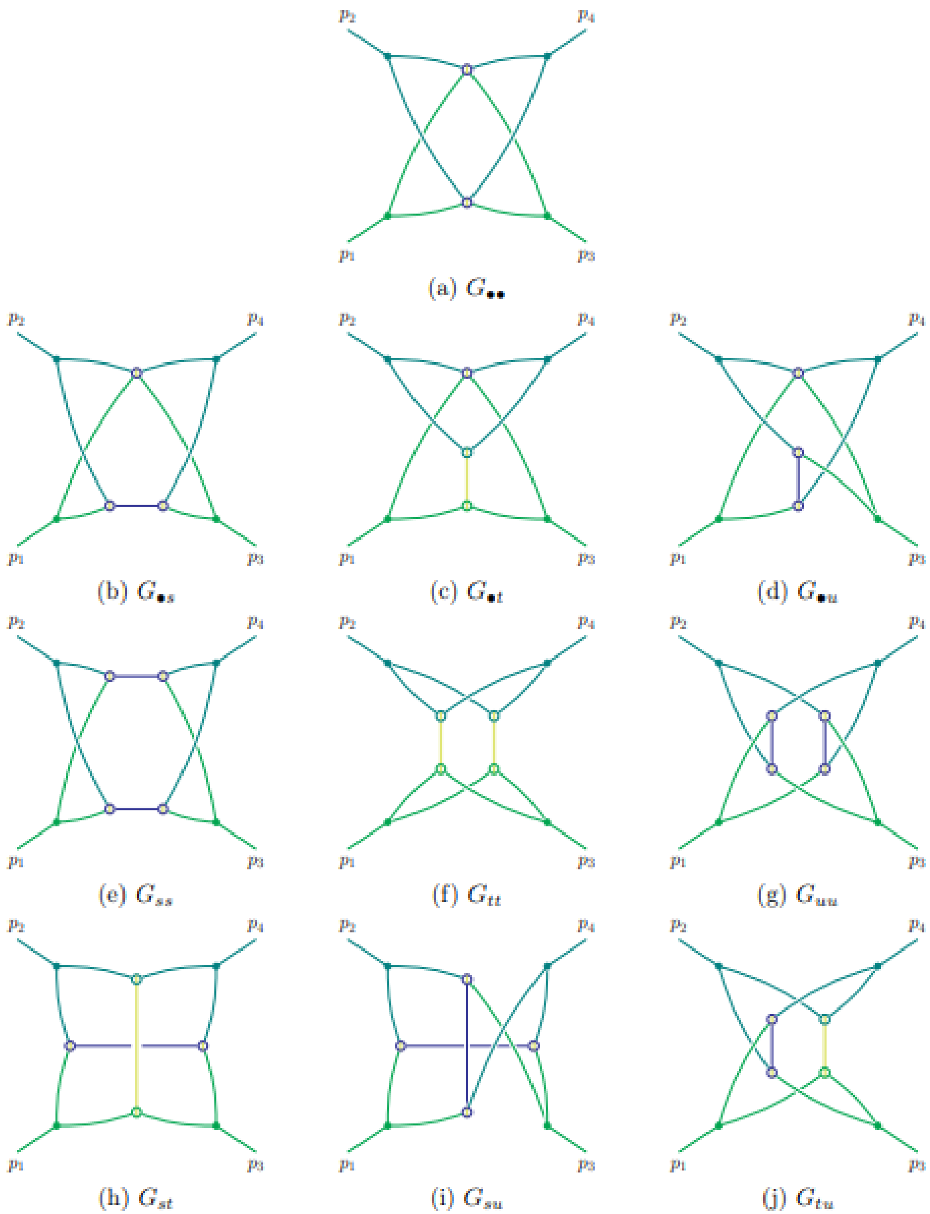


(a) $G_{\bullet\bullet}$ (b) $G_{\bullet s}$ (c) $G_{\bullet t}$ (d) $G_{\bullet u}$ (e) $G_{ss}$ (f) $G_{tt}$ (g) $G_{uu}$ (h) $G_{st}$ (i) $G_{su}$ (j) $G_{tu}$

# Main conclusions

The regions corresponding to a given graph can be predicted from the infrared picture!

– on–shell expansion: hard, collinear, soft.

– soft expansion: hard, collinear, soft.

– mass expansion: hard, collinear, soft, semihard, soft·collinear, soft$^2$•collinear, semicollinear, ...

– high–energy expansion: hard, collinear, soft, Glauber, soft •collinear, ...

with the mode interactions in certain patterns.

To identify facet regions – graph theoretical approach;

To identify hidden regions – dissecting the polytope.

# Outlook

Hopefully, this work can be helpful to the following aspects.

1. SCET, Glauber-SCET, SCET gravity, etc.
2. Phase space integrals.
3. Local infrared subtractions.
4. Can one even justify the method of regions with the help of our results?
5. Landau analysis of singularities.
6. Mathematical studies of convex/tropical geometry, etc.

…

# *Outlook*

Hopefully, this work can be helpful to the following aspects.

1. SCET, Glauber-SCET, SCET gravity, etc.
2. Phase space integrals.
3. Local infrared subtractions.
4. Can one even justify the method of regions with the help of our results?
5. Landau analysis of singularities.
6. Mathematical studies of convex/tropical geometry, etc.

…

THANK YOU!

# Backup slides

# *Identifying regions from Newton polytopes*

Back to our example:

Each region (hard, collinear-1, collinear-2, soft) corresponds to a specific facet containing certain points.

$$\mathcal{P}(\boldsymbol{x},\boldsymbol{s}) = x_1 + x_2 + x_3 - p_1^2 x_1 x_3 - p_2^2 x_2 x_3 - q_1^2 x_1 x_2$$

$x_1 \to$ (1,0,0;0), $x_2 \to$ (0,1,0;0), $x_3 \to$ (0,0,1;0), $p_1^2 x_1 x_3 \to$ (1,0,1;1), $p_2^2 x_2 x_3 \to$ (0,1,1;1), $q_1^2 x_1 x_2 \to$ (1,1,0;0)

These points are in the hard facet, with $\boldsymbol{v}_h$ = (0,0,0;1).

In comparison,

$$\textbf{Hard region}: \ \boldsymbol{x_1, x_2, x_3} \sim \boldsymbol{\lambda}^0$$

# *Identifying regions from Newton polytopes*

Back to our example:

Each region (hard, collinear-1, collinear-2, soft) corresponds to a specific facet containing certain points.

$$\mathcal{P}(\boldsymbol{x},\boldsymbol{s}) = x_1 + x_2 + x_3 - p_1^2 x_1 x_3 - p_2^2 x_2 x_3 - q_1^2 x_1 x_2$$

**(1,0,0;0)** **(0,0,1;0)** **(1,0,1;1)** **(1,1,0;0)**

These points are in the collinear-1 facet, with $\boldsymbol{v}_{C1}$ **= (-1,0,-1;1)**.

$$\textbf{Collinear region to } \boldsymbol{p_1}: \; \boldsymbol{x_1, x_3 \sim \lambda^{-1}}, \; \boldsymbol{x_2 \sim \lambda^{0}}$$

# *Identifying regions from Newton polytopes*

Back to our example:

Each region (hard, collinear-1, collinear-2, soft) corresponds to a specific facet containing certain points.

$$\mathcal{P}(\boldsymbol{x},\boldsymbol{s}) = x_1 + x_2 + x_3 - p_1^2 x_1 x_3 - p_2^2 x_2 x_3 - q_1^2 x_1 x_2$$

**(0,1,0;0)** **(0,0,1;0)** **(0,1,1;1)** **(1,1,0;0)**

These points are in the collinear-2 facet, with **$v_{C2}$ = (0,-1,-1;1)**.

$$\textbf{Collinear region to } p_2: \; x_1 \sim \lambda^0, \; x_2, x_3 \sim \lambda^{-1}$$

# *Identifying regions from Newton polytopes*

Back to our example:

Each region (hard, collinear-1, collinear-2, soft) corresponds to a specific facet containing certain points.

$$\mathcal{P}(\boldsymbol{x},\boldsymbol{s}) = x_1 + x_2 + x_3 - p_1^2 x_1 x_3 - p_2^2 x_2 x_3 - q_1^2 x_1 x_2$$

$x_3$ → **(0,0,1;0)**

$-p_1^2 x_1 x_3$ → **(1,0,1;1)**

$-p_2^2 x_2 x_3$ → **(0,1,1;1)**

$-q_1^2 x_1 x_2$ → **(1,1,0;0)**

These points are on the soft facet, with ***v**s* **= (-1,-1,-2;1)**.

$$\textbf{Soft region}: \; x_1, x_2 \sim \lambda^{-1}, \; x_3 \sim \lambda^{-2}$$

# Infrared structures of wide-angle scattering

- **Generic infrared divergences (pinch surfaces):**

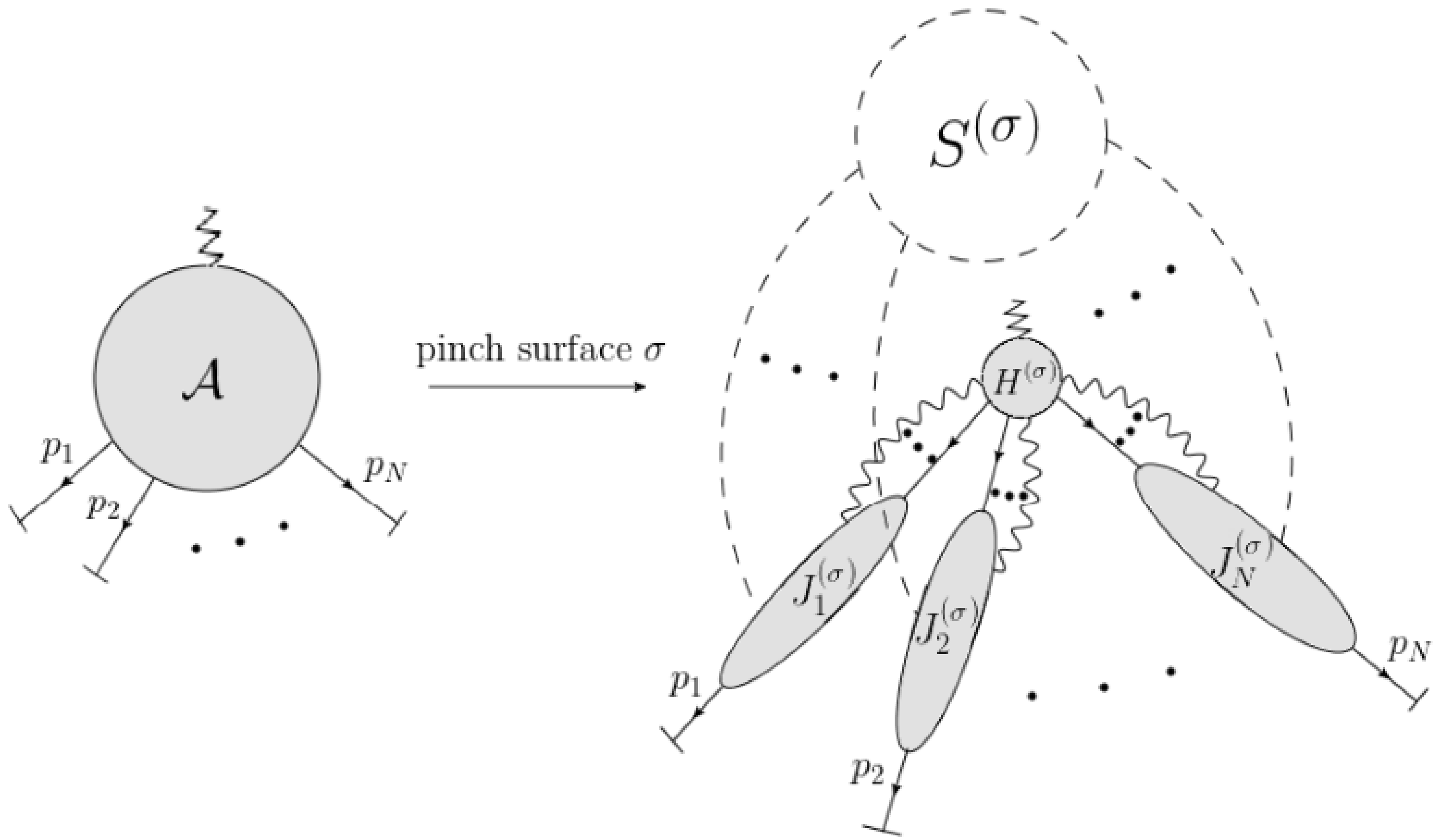


**This picture can be obtained from the Landau equations.**

# Infrared structures of wide-angle scattering

- **The Landau equations**

$$\alpha_e l_e^2(k,p,q) = 0 \qquad \forall e \in G$$
$$\frac{\partial}{\partial k_a}\mathcal{D}\left(k,p,q;\alpha\right) = 0 \qquad \forall a \in \{1,\ldots,L\}\,.$$

**are necessary conditions for infrared singularity. The solutions of the Landau equations are called pinch surfaces.**

- **The pinch surfaces of hard processes has been studied in detail in the past decades.**

- **Motivation: it looks that the infrared regions are in one-to-one correspondence with the pinch surfaces!**

# *Regions in the on–shell expansion*

E.Gardi, F.Herzog, S.Jones, YM, J.Schlenk, JHEP07(2023)197

- **Each solution of the Landau equations corresponds to a region, provided that some requirements of H, J, and S are satisfied.**

  - *Requirement of $H$: all the internal propagators of $H_{\mathrm{red}}$, which is the reduced form of $H$, are off-shell.*
  - *Requirement of $J$: all the internal propagators of $\widetilde{J}_{i,\mathrm{red}}$, which is the reduced form of the contracted graph $\widetilde{J}_i$, carry exactly the momentum $p_i^\mu$.*
  - *Requirement of $S$: every connected component of $S$ must connect at least two different jet subgraphs $J_i$ and $J_j$.*

# *Idea of the proof*

For the Symanzik polynomials,

$$\mathcal{U}(\boldsymbol{x}) = \sum_{T^1} \prod_{e \notin T^1} x_e, \qquad \mathcal{F}(\boldsymbol{x};\boldsymbol{s}) = -\sum_{T^2} s_{T^2} \prod_{e \notin T^2} x_e + \mathcal{U}(\boldsymbol{x}) \sum_e m_e^2 x_e \,.$$

- The terms are described by **spanning (2-)trees** of $G$.
- Furthermore, the terms are described by **weighted spanning (2-) trees** of $G$ for a given scaling of the parameters.
- The **leading** terms are described by the **minimum spanning (2-) trees** of $G$.

Graph theory

- Meanwhile, regions ←→ lower facets of the Newton polytope.

Convex geometry

# *The proof*

- Long and technical.

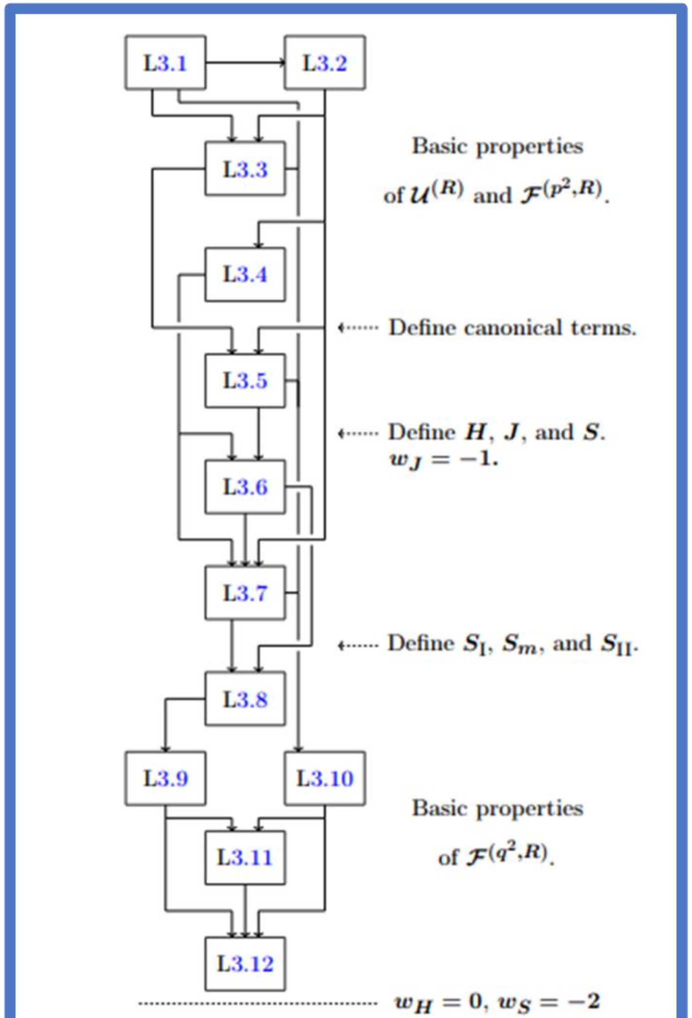


12 lemmas, ~50 pages...

- It works exclusively for the on-shell expansion, but can be slightly modified to apply to some other expansions.

# *Regions vs singularities*

Edges expanding at different relative rates

$$\rho, \lambda, \sigma \to \infty$$

$$\zeta, \delta, \xi \to \infty$$

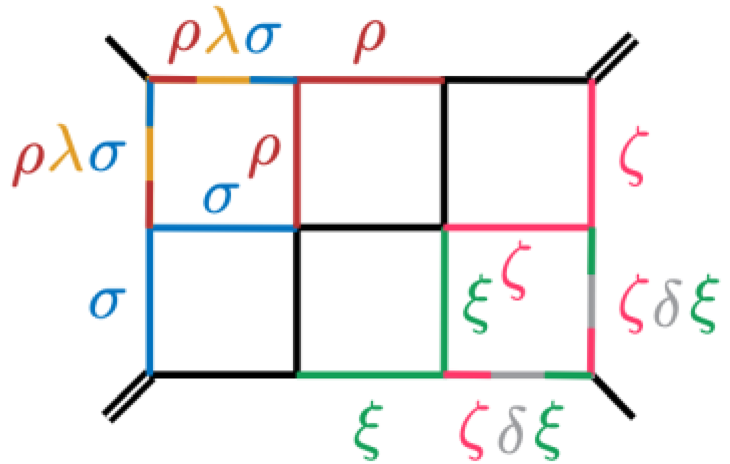


(Arkani-Hamed, Hillman, Mizera, 2022)

*A pinch singularity residing in the double-collinear region.*

# *A graph–finding algorithm*

- Based on this conclusion, we can construct a **graph-finding algorithm** to unveil all the regions.
- A fishnet example

**Step 1: constructing the "primitive jets":**

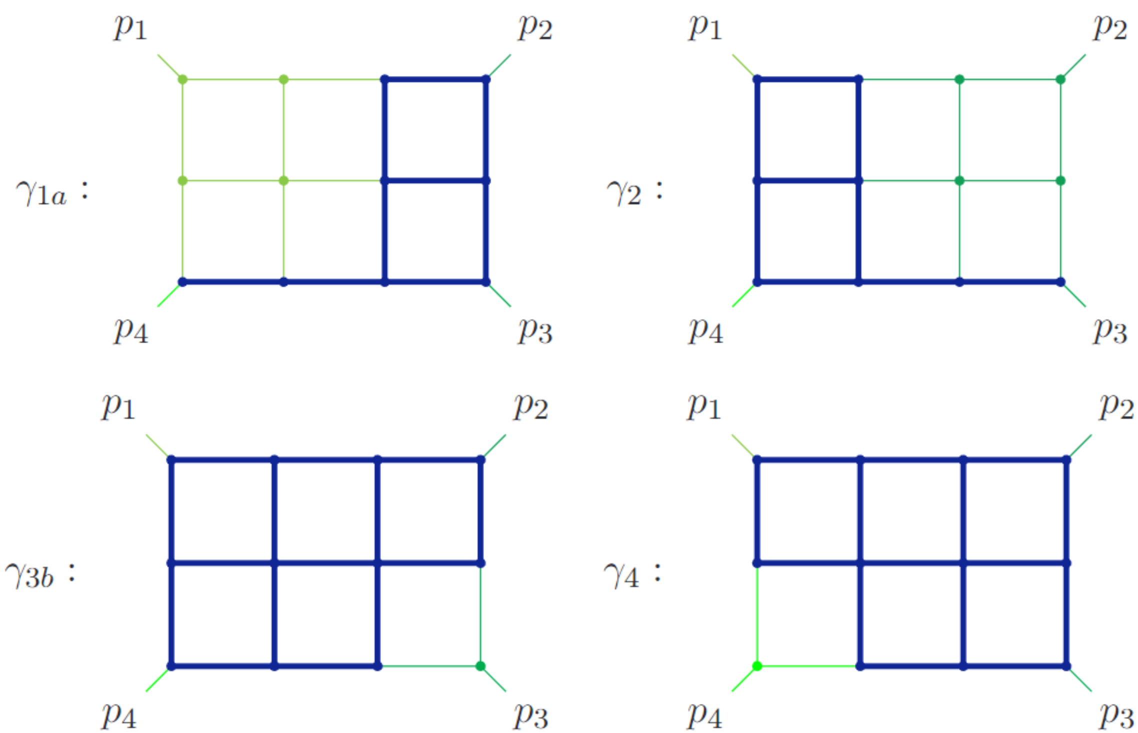


E.Gardi, F.Herzog, S.Jones, YM, J.Schlenk, JHEP07(2023)197

# *A graph–finding algorithm*

- Based on this conclusion, we can construct a **graph-finding algorithm** to unveil all the regions.
- A fishnet example

**Step 2: overlaying the "primitive jets":**

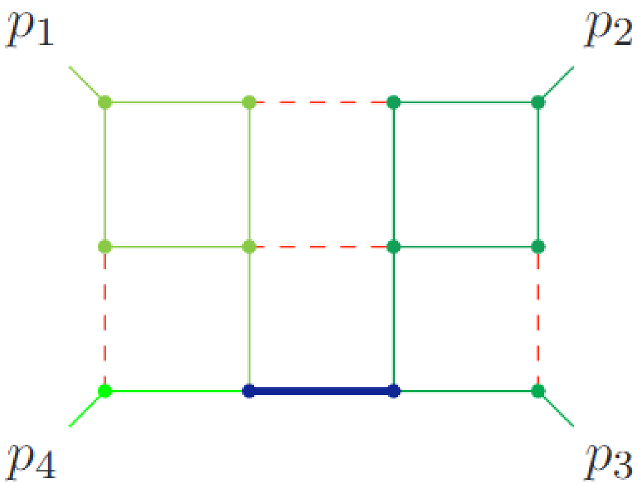


**Step 3: removing pathological configurations.**

This algorithm does not involve constructing Newton polytopes, and can be much faster.

E.Gardi, F.Herzog, S.Jones, YM, J.Schlenk, JHEP07(2023)197

# *Application 2: analytic structures of $\mathcal{I}$*

- In addition, one can use this knowledge to study the analytic structure of wide-angle scattering, which further leads to properties regarding the commutativity of multiple on-shell expansions.

**Theorem 4.** *If $R$ is a jet-pairing soft region that appears in the on-shell expansion of a wide-angle scattering graph $G$, then the all-order expansion of $\mathcal{I}(G)$ in this region can be written as follows:*

$$\mathcal{T}_{\boldsymbol{t}}^{(R)}\mathcal{I}(\boldsymbol{s}) = \bigg(\prod_{p_i^2\in\boldsymbol{t}} (p_i^2)^{\rho_{R,i}(\epsilon)}\bigg) \cdot \sum_{k_1,\ldots,k_{|\boldsymbol{t}|}\geqslant 0} \bigg(\prod_{p_i^2\in\boldsymbol{t}} (-p_i^2)^{k_i}\bigg) \cdot \overline{\mathcal{I}}_{\{k\}}^{(R)}(\boldsymbol{s}\setminus\boldsymbol{t})\,, \tag{5.8}$$

*where $\rho_{R,i}(\epsilon)$ is a linear function of $\epsilon$, $k_i$ are non-negative integer powers and $\overline{\mathcal{I}}_{\{k\}}^{(R)}(\boldsymbol{s}\setminus\boldsymbol{t})$ is a function of the off-shell kinematics, independent of any $p_i^2\in\boldsymbol{t}$.*

# *Landau analysis of cancellations*

- Each region (except the hard region) must correspond to an infrared singularity, satisfying the Landau equations:

$$\mathcal{F}(\boldsymbol{\alpha}; \boldsymbol{s}) = 0,$$
$$\forall i, \quad \alpha_i = 0 \ \text{ or } \ \partial\mathcal{F}/\partial\alpha_i = 0.$$

- Therefore, $\mathcal{F}$ having both positive and negative terms does not necessarily imply a region, because the Landau equation above may not be satisfied.
- For example,

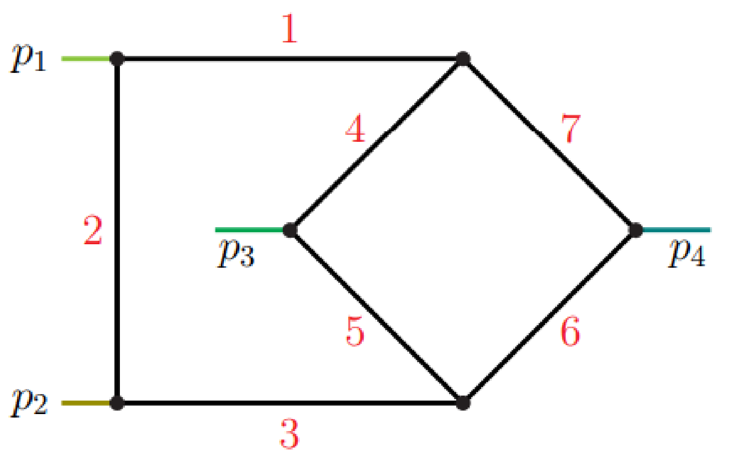

# *Landau analysis of cancellations*

- For example,

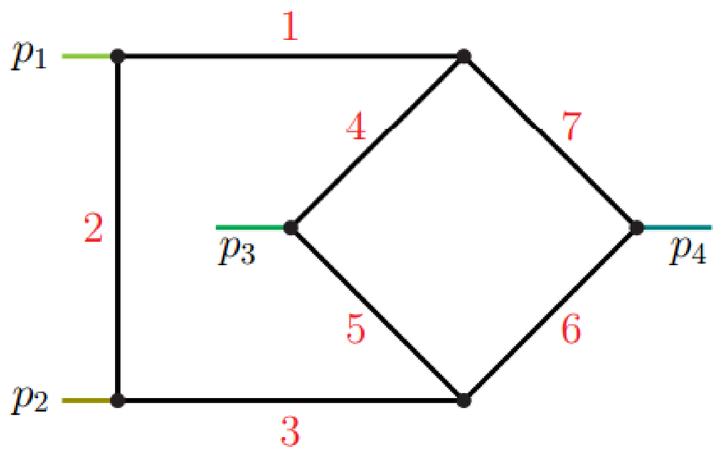


$$
\begin{aligned}
\mathcal{F}(\boldsymbol{\alpha};\boldsymbol{s}) = \quad & (-p_1^2)\left[\alpha_1\alpha_2(\alpha_4+\alpha_5+\alpha_6+\alpha_7)+\alpha_2\alpha_4\alpha_7\right] \\
& +(-p_2^2)\left[\alpha_2\alpha_3(\alpha_4+\alpha_5+\alpha_6+\alpha_7)+\alpha_2\alpha_5\alpha_6\right] \\
& +(-p_3^2)\left[\alpha_4\alpha_5(\alpha_1+\alpha_2+\alpha_3+\alpha_6+\alpha_7)+\alpha_1\alpha_5\alpha_7+\alpha_3\alpha_4\alpha_6\right] \\
& +(-p_4^2)\left[\alpha_6\alpha_7(\alpha_1+\alpha_2+\alpha_3+\alpha_4+\alpha_5)+\alpha_1\alpha_4\alpha_6+\alpha_3\alpha_5\alpha_7\right] \\
& +(-q_{12}^2)\left[\alpha_1\alpha_3(\alpha_4+\alpha_5+\alpha_6+\alpha_7)+\alpha_3\alpha_4\alpha_7+\alpha_1\alpha_5\alpha_6\right] \\
& +(-q_{13}^2)\alpha_2\alpha_5\alpha_7+(-q_{14}^2)\alpha_2\alpha_4\alpha_6.
\end{aligned}
$$

# *Landau analysis of cancellations*

- For example,

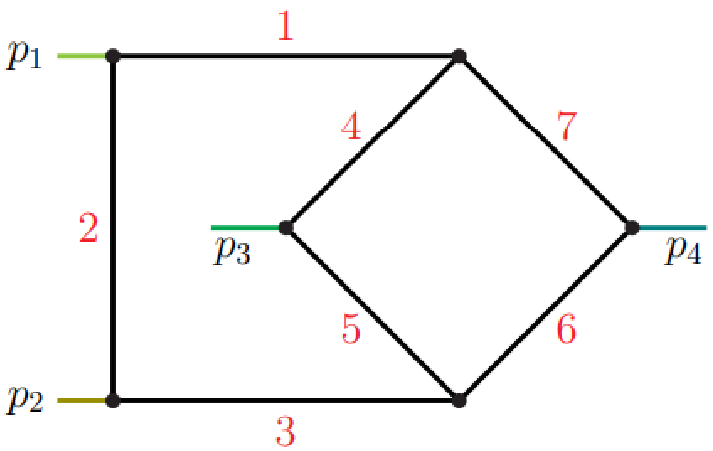


One can check that any possible cancellation within $\mathcal{F}$ is not compatible with the Landau equations.

- Therefore, all the regions are from the lower facets of the Newton polytope.

- Actually, as one can check in this way, most cases where $\mathcal{F}$ is indefinite does not have regions due to cancellations.

# ***High–energy expansion of forward scattering***

Consider the Regge limit of the 2-to-2 forward scattering.

Regions include:

hard, collinear, soft, *Glauber*, soft·collinear, collinear$^3$, …

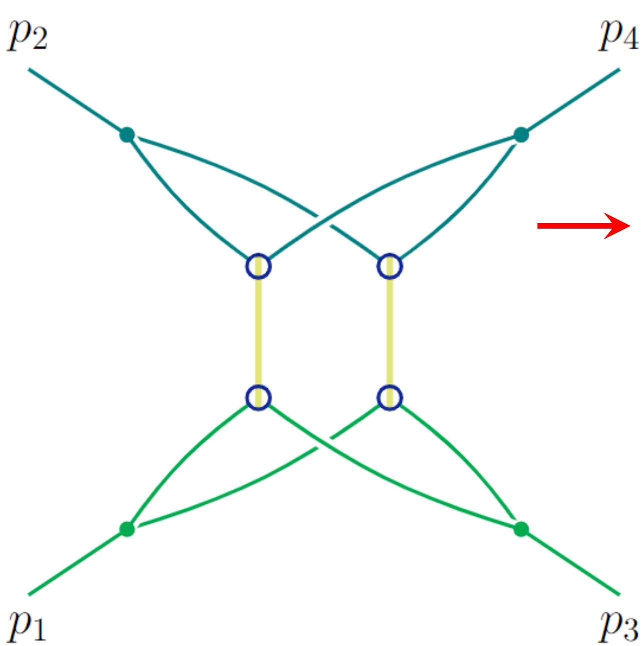


**From 3 loops.**

**Not facets of the Newton polytope.**
**Due to the cancellation of the following terms**

$$s_{12}\cdot(x_1x_4 - x_2x_3)\cdot(x_5x_8 - x_6x_7).$$

**Cannot be detected by Asy2 either.**

**Much more to explore!**

E.Gardi, F.Herzog, S.Jones, YM, JHEP08(2024)127

# Some old references


1. Nambu, 1957, *Parametric Representations of General Green's Functions.*
2. Amati, Stanghellini, Fubini, 1962, *Asymptotic properties of scattering and multiple production*.
3. Islam, Landshoff, Taylor, 1963, *Singularity of the Regge amplitude*.
4. Mandelstam, 1963, *Cuts in the angular-momentum plane.*
5. Halliday, 1963, *High-energy behavior of perturbation Theory.*
6. Tiktopolous, 1963, *High-energy behavior of Feynman amplitudes*.
7. Halliday, 1964, *High energy behavior at fixed angle in perturbation theory*.
8. Menke, 1964, *High-energy behaviour of Feynman integrals involving singular configuration*.
9. Hamprecht, 1965, *High-energy behavior of Feynman amplitudes*.
10. Lam, 1968, *High-energy behaviour of Feynman diagrams via the electric-circuit analogy*.
11. Landshoff, 1974, *Model for elastic scattering at wide angle*.

…

# *Some old references*

ANNALS OF PHYSICS: **28**, 320–345 (1964)

## High Energy Behavior at Fixed Angle in Perturbation Theory*

I. G. HALLIDAY

*Department of Applied Mathematics and Theoretical Physics, University of Cambridge, Cambridge, England*

The high energy behavior of the planar diagrams in a $g\phi^3$ theory at fixed angle is shown to be dominated by the Born terms. The behavior of the ladder diagrams is calculated in detail. It is then shown that the graphs possessing third spectral functions which give rise to the Gribov-Pomeranchuk singularity and Regge cuts behave like $s^{-5/2}$ as $s \to \infty$ at fixed angle. A set of planar diagrams is also investigated whose behavior on an unphysical sheet is prevented from breaking the Born behavior only by the existence of the Froissart bound. Finally the Bjorken-Wu graphs are shown to behave like $\log^2 s/s$ for all orders.

# *Some old references*

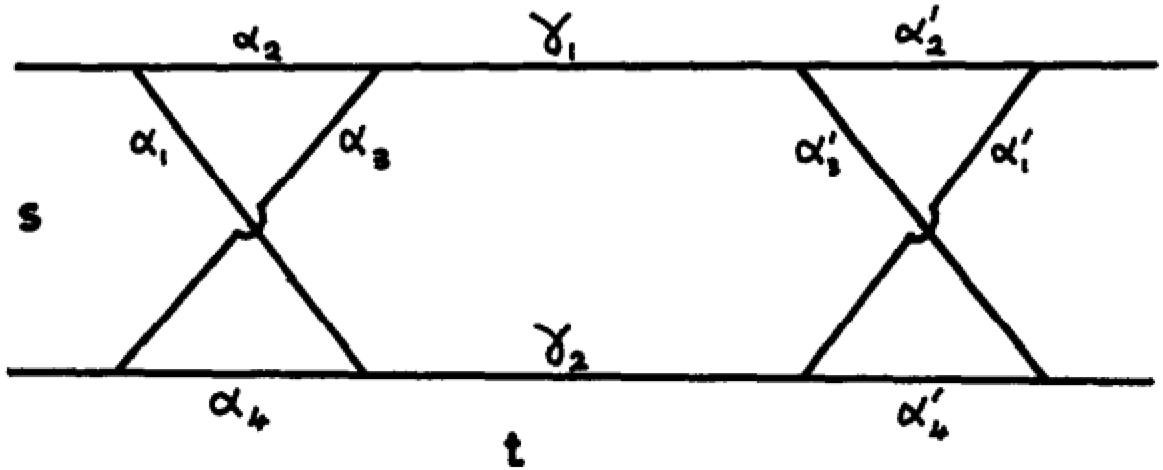

# Some old references

In the limit $t \to \infty$ with $s$ fixed the graph of Fig. 4 behaves like $1/t^8$ and contributes towards the Gribov-Pomeranchuk singularity at $l = -1$. Further iterations give rise to terms $1/t \cdot (\log t)^{n-2}$. For this graph

$$g = (\alpha_1\alpha_3 - \alpha_2\alpha_4)(\alpha_1'\alpha_3' - \alpha_2'\alpha_4') \tag{27}$$

$$\begin{aligned} f = & -\alpha_2\alpha_4\cdot\alpha_1'\alpha_3' - \alpha_1\alpha_3\alpha_2'\alpha_4' \\ & + \gamma_1\gamma_2(\alpha_1 + \alpha_2 + \alpha_3 + \alpha_4)(\alpha_1' + \alpha_2' + \alpha_3' + \alpha_4') \\ & + \gamma_1[\alpha_1\alpha_4(\alpha_1' + \alpha_2' + \alpha_3' + \alpha_4') + \alpha_1'\alpha_4'(\alpha_1 + \alpha_2 + \alpha_3 + \alpha_4)] \\ & + \gamma_2[\alpha_2\alpha_3(\alpha_1' + \alpha_2' + \alpha_3' + \alpha_4') + \alpha_2'\alpha_3'(\alpha_1 + \alpha_2 + \alpha_3 + \alpha_4)] \\ & + \alpha_3'\alpha_2'\alpha_1\alpha_4 + \alpha_1'\alpha_4'\alpha_2\alpha_3 . \end{aligned} \tag{28}$$

If we now let $x = \alpha_1\alpha_3 - \alpha_2\alpha_4$ and $y = \alpha_1'\alpha_3' - \alpha_2'\alpha_4'$ then the $x$, $y$ integrations give rise to a pinch of the integration contour and when we integrate over $x$, $y$ we obtain the form (II Eq. (9))

$$\int \frac{\delta(\alpha_1\alpha_3 - \alpha_2\alpha_4)\delta(\alpha_1'\alpha_3' - \alpha_2'\alpha_4')\Delta^2 \prod d\xi\delta\left(\sum \xi - 1\right)}{ks[fs + d]^3} . \tag{29}$$

# *Local infrared subtractions*

- Aim: construct counterterms removing both IR and UV singularities at the level of **integrand**.

- We need the “hard-collinear” and “soft-collinear” approximations that are exactly used for the method of regions.

- Main differences: ① no hard region. ② more nested approx.

- Technical difficulties in local subtractions:
  - Power divergences.
  - Spurious polarization for factorization (“loop polarizations”).
  - Momentum shift mismatch from the Ward identities.

# *Local infrared subtractions*

- Aim: construct counterterms removing both IR and UV singularities at the level of **integrand**.

- We need the "hard-collinear" and "soft-collinear" approximations that are exactly used for the method of regions.

- Main differences: ① no hard region. ② more nested approx.

- Recent progresses at two loops:

- 2-loop 2→2 wide-angle scattering (Anastasiou & Sterman 2018)
- 2-loop $e^+e^- \to W, Z, \gamma^*$ (Anastasiou, Haindl, Sterman, Yang, Zeng 2020)
- 2-loop $q\bar{q} \to W, Z, \gamma^*$ (Anastasiou & Sterman 2022)
- 2-loop $gg \to h \cdots h$ (Anastasiou, Karlen, Sterman, Venkata 2023)